

AD-A093 316

IBM THOMAS J WATSON RESEARCH CENTER YORKTOWN HEIGHTS NY
CHEMICAL REACTIONS AT THE METAL/SILICON INTERFACE.(U)

F/6 7/3

OCT 80 G W RUBLOFF, P S HO, T Y TAN

N00014-79-C-0932

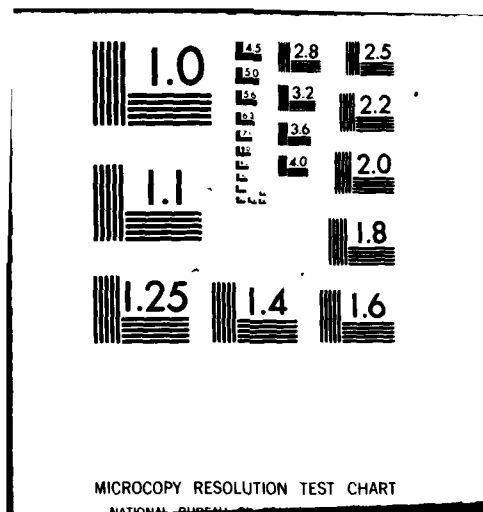
NL

UNCLASSIFIED

For 1
00.0



11



CHEMICAL REACTIONS AT THE METAL/SILICON INTERFACE

LEVEL

II

G. W. Rubloff, P. S. Ho, and T. Y. Tan

IBM Thomas J. Watson Research Center

P. O. Box 218, Yorktown Heights, New York 10598

October 31, 1980

Final Report for period 1 August 1979 - 31 October 1980

Contract N00014-79-C-0932

Sponsored by Office of Naval Research

DTIC
ELECT
S **DEC 19 1980**
F

Approved for public release; distribution unlimited.

Reproduction in whole or part is permitted for any purpose of the United States Government.

DDC FILE COPY

80 12 18 051

Unclassified

SECURITY CLASSIFICATION OF THIS PAGE (When Data Entered)

REPORT DOCUMENTATION PAGE		READ INSTRUCTIONS BEFORE COMPLETING FORM
1. REPORT NUMBER	2. GOVT ACCESSION NO.	3. RECIPIENT'S CATALOG NUMBER
	AD-A093316	
4. TITLE (and Subtitle)	5. TYPE OF REPORT & PERIOD COVERED	
(6) Chemical Reactions at the Metal/Silicon Interface	(9) Final Report. 1 August 1979-Oct 1979	
7. AUTHOR(s)	8. PERFORMING ORG. REPORT NUMBER	
(10) G.W. Rubloff / P.S. Ho and T.Y. Tan	(31)	
9. PERFORMING ORGANIZATION NAME AND ADDRESS	10. PROGRAM ELEMENT, PROJECT, TASK AREA & WORK UNIT NUMBERS	
IBM T.J. Watson Research Center P.O. Box 218, Yorktown Heights, N.Y. 10598		
11. CONTROLLING OFFICE NAME AND ADDRESS	12. REPORT DATE	
Office of Naval Research 800 N. Quincy St. Arlington, Virginia 22217	(11) 31 October 1980	
14. MONITORING AGENCY NAME & ADDRESS (if different from Controlling Office)	13. NUMBER OF PAGES	
(12) 96		
15. SECURITY CLASS. (of this report)		16. DISTRIBUTION STATEMENT (of this Report)
Unclassified		Approved for public release: distribution unlimited
17. DISTRIBUTION STATEMENT (of the abstract entered in Block 20, if different from Report)		
18. SUPPLEMENTARY NOTES		
19. KEY WORDS (Continue on reverse side if necessary and identify by block number)		
Interfaces, electronic and atomic structure, silicides, silicide formation, interface states.		
→ THIS REPORT INCLUDES THE		
20. ABSTRACT (Continue on reverse side if necessary and identify by block number)		
The accomplishments of the work performed under the contract entitled "Chemical Reactions at the Metal/Silicon Interface" are summarized. Included are studies of Si(111) and Si(100) surfaces with Pd, Pt, Ni, and V metal overlayers leading to silicide formation. Experimental techniques utilized include ultraviolet photoemission spectroscopy, Auger electron spectroscopy, work function measurements and transmission electron microscopy.		

DD FORM 1 JAN 73 1473 EDITION OF 1 NOV 68 IS OBSOLETE

Unclassified

SECURITY CLASSIFICATION OF THIS PAGE (When Data Entered)

349250 HWE

I. Initial Proposal

IBM proposed a one-year best efforts experimental study of the initial stages of chemical reaction at the metal/Si interface. The study was aimed at acquiring a fundamental understanding of microscopic mechanisms responsible for silicide and Schottky barrier formation. To provide a comprehensive picture of the microscopic interface phenomena and properties, the experimental work was directed into three areas: (1) interface electronic structure, (2) interface atomic structure, and (3) interface electrical properties. A three-month no-cost extension of the contract was made to complete data analysis and manuscript preparation.

Accession For	
NTIS GRA&I	<input checked="checked" type="checkbox"/>
DTIC TAB	<input type="checkbox"/>
Unannounced	<input type="checkbox"/>
Justification	
By	
Distribution/	
Availability Codes	
Dist	Avail and/or Special
A	

II. Accomplishments under the Project

A significant portion of the work completed under the contract has been published or is available in preprint form. Other results remain to be written and published. In the following we briefly summarize the accomplishments of this research. These accomplishments are:

- (1) Silicide compound formation (Pd_2Si) dominates the microscopic chemistry and properties of the atomically clean Pd/Si interface. Identification of this chemistry permits for the first time a close evaluation of the nature of electronic states at a metal/semiconductor interface. Thus the interface electronic structure is primarily that of the bulk silicide compound formed. (Refs. 1-4)
- (2) Reactivity at the Pd/Si interface is very high, with compound formation occurring spontaneously at room or even at low temperatures (down to 180°K). (Refs. 1-4)
- (3) The electronic properties of a bulk silicide have been understood from experiment and theory for the first time. Chemical bonding in Pd_2Si occurs by essentially covalent bonds between Pd(4d) and Si(3p) states, which form bonding bands ~5 eV below the Fermi energy and antibonding bands near the Fermi energy. Occupancy of the latter determines phase stability of Pd-Si mixtures. The main portion of Pd(4d) states, not involved in Pd-Si bonding, are located well below the Fermi energy (by ~3 eV), producing an electronic structure more like that of a noble metal than of a transition metal. (Ref. 5)
- (4) Chemical shifts of spectral features in photoemission and Auger spectra occur with changing metal coverage from the submonolayer range up and reflect the altered environment of atoms near the interface. These effects are suggestive

of stoichiometry variations in the silicide near the interface and form the basis for a new theory of silicide Schottky barrier heights. (Refs. 1-6)

- (5) Silicide compound formation also dominates the electronic structure of the Pt/Si interface; however, chemical shift phenomena are much smaller. (Ref. 3)
- (6) Photoemission and Auger spectra show that the density-of-states near the Fermi energy (i.e., in the Si band gap region) is enhanced at low metal coverage, indicating that electronic states exist in this region only near the interface; these may be associated with true interface states, localized bonding configurations characteristic of the interface, or defect states resulting from the interface reactivity, and they represent interface electronic structure contributions additional to those of the bulk silicide reaction product. The interface-associated states occur in relatively high density (of order 0.1 per interface atom) and a considerable fraction of them are localized partly on the Si atoms at the interface. (Refs. 2-4)
- (7) Cross-sectional TEM measurements of Ni, Pd, and Pt silicide/Si interfaces show that the interface is atomically abrupt, with no amorphous layer structure present. Misfit dislocations and atomic steps are observed, and the degree of roughness on an atomic or macroscopic scale depends on whether epitaxy occurs, on lattice match, and on the extent of faceting. On a microscopic scale for epitaxial silicide/Si contacts, the interface can be atomically sharp and smooth, producing regular lattice fringes extending directly to the interface. This interface sharpness and the observation of interface electronic states provide a basis for constructing interface models which correlate interface atomic and electronic structure. (Ref. 7)

- (8) Detailed Auger composition analysis for the $\text{Pd}_2\text{Si}/\text{Si}$ interface indicates that the silicide is nearly stoichiometric except for a very thin ($\sim 3 \text{ \AA}$) Si-rich region just at the intimate interface. This character of this region is consistent with the chemical shift observations noted above. (Ref. 4)
- (9) Since electronic structure is probed mainly by surface-spectroscopy techniques, it is important to assure that the composition of the surface region near the vacuum interface is representative of the entire overlayer film. Techniques to check this have been developed. Surface segregation and enrichment phenomena in the near-noble-metal/Si interface systems have been identified, and their understanding is a prerequisite for reliable conclusions about interface behavior. For Ni, Pd, and Pt on Si annealing at temperatures above the silicide formation temperatures produces a thin (few monolayer) film of essentially elemental Si on top of the silicide (at the vacuum interface). (Refs. 2, 8)
- (10) The behavior of refractory-metal/Si interfaces is quite different from that at near-noble metal/Si interfaces. Reaction does not take place at the V/Si interface at room temperature, and silicide formation (VSi_2) does not begin until $\sim 500^\circ\text{C}$. However, at intermediate temperatures ($\sim 200\text{--}400^\circ\text{C}$) strong V-Si intermixing does occur as a precursor to silicide formation. (Ref. 3)

References

1. J. L. Freeouf, G. W. Rubloff, P. S. Ho, and T. S. Kuan, *Phys. Rev. Letters* **43**, 1836 (1979).
2. G. W. Rubloff, P. S. Ho, J. L. Freeouf, and J. E. Lewis, submitted to *Phys. Rev. B* **15**.
3. G. W. Rubloff, *Proc. of the 8th International Vacuum Congress, Cannes, France, Sept. 22-26, 1980, Vol. I, Thin Films*, p. 562.
4. P. S. Ho, H. Foll, J. E. Lewis, and P. E. Schmid, *Proc. of the 4th Int. Conf. on Solid Surfaces and the 3rd European Conf. on Surface Science, Cannes, France, Sept. 22-26, 1980, Vol. II*, p. 1376.
5. P. S. Ho, G. W. Rubloff, J. E. Lewis, V. L. Moruzzi, and A. R. Williams, to be published in *Phys. Rev. B* **15** (Nov. 1980).
6. J. L. Freeouf, *Solid State Commun.* **33**, 1059 (1980).
7. H. Foll, P. S. Ho, and K. N. Tu, to be published in *J. Appl. Phys.*.
8. J. L. Freeouf, G. W. Rubloff, P. S. Ho, and T. S. Kuan, *J. Vac. Sci. Technol.* **17**, 916 (1980).

III. Personnel involved in contract work:

G. W. Rubloff - principal co-investigator

P. S. Ho - principal co-investigator

T. Y. Tan - principal co-investigator

J. E. Lewis

P. E. Schmid

J. G. Clabes

H. Foll

K. N. Tu

IV. Appendix

To date the following papers have been written and submitted for publication under the contract:

- Item 1. Reprint, "Photoemission Studies of Chemical Bonding and Reactions at the Metal/Silicon Interface", G. W. Rubloff, Proc. of the 8th International Vacuum Congress, Cannes, France, Sept. 22-26, 1980, Vol. I, Thin Films, p. 562.
- Item 2. Reprint, "Chemical Bonding and Microstructures of Metal/Si Interfaces During Silicide Formation", P. S. Ho, H. Foll, J. E. Lewis, and P. E. Schmid, Proc. of the 4th Int. Conf. on Solid Surfaces and the 3rd European Conf. on Surface Science, Cannes, France, Sept. 22-26, 1980, Vol. II, p. 1376.
- Item 3. Preprint, "Chemical Bonding and Electronic Structure of Pd_2Si ", P. S. Ho, G. W. Rubloff, J. E. Lewis, V. L. Moruzzi, and A. R. Williams, to be published in Phys. Rev. B15 (Nov. 1980).
- Item 4. Preprint, "Chemical Bonding and Reactions at the Pd/Si Interface", G. W. Rubloff, P. S. Ho, J. L. Freeouf, and J. E. Lewis, submitted to Phys. Rev. B15.
- Item 5. Preprint, "Cross-Sectional TEM of Silicon-Silicide Interfaces", H. Foll, P. S. Ho, and K. N. Tu, to be published in J. Appl. Phys..

PHOTOEMISSION STUDIES OF CHEMICAL BONDING AND REACTIONS AT THE METAL/SILICON INTERFACE*

G.W. Rubloff

IBM T.J. Watson Research Center, P.O. Box 218, Yorktown Heights, N.Y. 10598 USA

UPS studies of Pd/Si(100), Pt/Si(100), and V/Si(100) show evidence for interfacial compound formation, stoichiometry variations, and interface-associated electronic states in the Si band gap.

The microscopic chemistry and electronic structure of the metal/Si interface play a crucial role in the materials reactions and Schottky barrier properties of these technologically important contacts. Recent surface spectroscopy studies have begun to reveal the detailed phenomena which occur at these reactive interfaces. Here we present ultraviolet photoemission spectroscopy (UPS) results for Pd, Pt, and V on Si surfaces, which illustrate some of these phenomena, including compound formation [1,2], stoichiometry gradations [1,2], and interface-associated states in the gap [3].

The n-Si(100) samples were cleaned in UHV by ion bombardment and annealing (via resistive heating) at up to 850°C. The clean surfaces showed a c(4x2) LEED pattern. Metal overlayers were evaporated by direct sublimation from a resistively heated pure metal wire, with relative coverages determined by use of a shutter to control deposition times for fixed evaporation conditions. Metal coverages were calibrated by a quartz microbalance and by Auger composition analysis and are given in terms of equivalent metal thickness.

Angle-integrated UPS results (He I spectra, $h\nu = 21.2\text{ eV}$) for Pd/Si(100) are depicted in Fig. 1. The clean Si(100) spectrum (Fig. 1a) shows bulk Si features and also intrinsic surface state features near -0.7 and -1.3 eV [4] referenced to zero at the Fermi energy E_F . Upon deposition of thin (submonolayer) Pd overlayers, the emission intensity grows due to the large Pd(4d) UPS cross-section. The coverage-dependent change in the spectra is indicated by the incremental difference curves (Figs. 1b, 1c, and 1d), which give the change in emission caused by successive metal depositions of $\sim 0.25\text{ \AA}$. The total spectra for $\sim 4\text{ \AA}$ and $\sim 12\text{ \AA}$ Pd deposited at 25°C are shown in Figs. 1e and 1f. The spectrum in Fig. 1f is that of the silicide compound Pd_2Si , as identified by in-situ Auger analysis and (after removal from the UHV system) by TEM phase analysis [1,2].

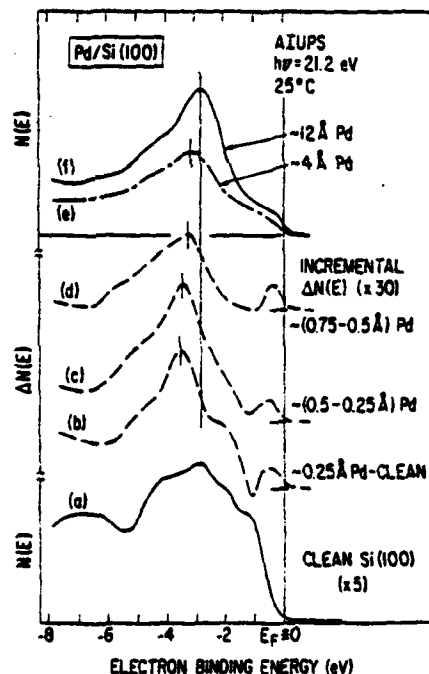


Fig. 1. Pd/Si(100) UPS results: (a) spectrum for clean Si(100); (b)-(d) incremental difference spectra for Pd/Si(100); (e), (f) spectra for Pd on Si(100). Fig. 1f is essentially the spectrum for the Pd_2Si compound.

Compound formation thus occurs spontaneously at 25°C on the clean surface. The main Pd(4d) bands lie between -5 and -2 eV, i.e. well below E_F as in the noble metals. Chemical bonding of Pd₂Si occurs via bonding and antibonding Pd(4d)-Si(3p) states near -6.5 eV and -1 eV respectively [5].

At lower (Fig. 1e) and at submonolayer (Figs. 1b-1d) coverages, the electronic structure has the same overall shape as that of Pd₂Si. (In the low-coverage difference curves between -2 and -0.5 eV this similarity is somewhat masked by spectral structure arising from the metal-induced quenching of intrinsic surface states). Since this similarity is also observed for the L_{2,3} VV Auger spectrum (which reflects the Si local density-of-states) [2], we conclude that formation of a Pd₂Si-like compound occurs at the interface and dominates the microscopic chemistry and electronic properties of the interface.

The shift of the main Pd(4d) peak with coverage is attributed to changes in the stoichiometry (and/or chemical environment for very low coverages) of the Pd₂Si-like bonds with distance from the interface [1,2]. This interpretation is consistent [5] with stoichiometry-dependent trends found in theoretical calculations and in experimental results for the Pd_{1-x}Si_x metallic glasses. Related shifts are observed in the Si L_{2,3} VV Auger spectra. The UPS shifts suggest that the Pd₂Si-like material is effectively Si-rich near the interface, an interpretation which has led to a new approach to understanding silicide Schottky barrier heights [6].

Results for Pt/Si(100) are shown in Fig. 2. The low-coverage difference spectra (Figs. 2b-2f) are very similar in shape to that of the silicide formed at $\leq 200^\circ\text{C}$ on the clean Si surface (see Fig. 2g). Although our temperature-dependent investigations indicate clearly that this spectrum is characteristic of the initial silicide phase produced at these temperatures, we have not determined whether this interface phase is PtSi or Pt₂Si; thin film studies of thicker Pt layers on clean Si show initial Pt₂Si formation followed by conversion to the end product PtSi at higher temperatures [7]. In either case, silicide formation dominates the chemistry and electronic properties of the interface. In contrast to the behavior for Pd/Si(100), the low-coverage Pt/Si(100) spectra show no significant shift of the d-band doublet peaks (near -3.5 and -5.5 eV) with coverage. This suggests that stoichiometry variations (Si enrichment) of the silicide at the interface are smaller for Pt/Si(100) than for Pd/Si(100).

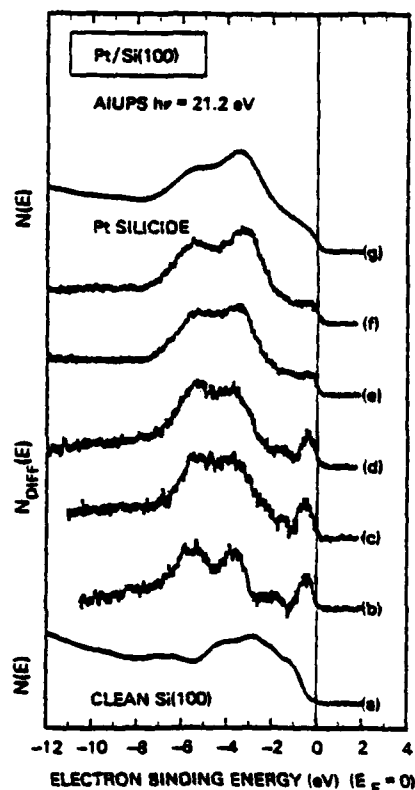


Fig. 2. Pt/Si(100) results: (a) spectrum for clean Si(100); (b)-(f) incremental difference spectra for Pt/Si(100), shown in expanded scale for ~ 0.25 - 0.5\AA coverage increments; (g) spectrum for initial Pt silicide phase formed by 200°C annealing after 25°C deposition.

Since the silicides produced at the interface are metals, they give electronic states near E_F , i.e. in the Si band gap region crucial in determining the electrical properties of the contact. However, Fig. 2 shows that the density-of-states just below E_F (from -0.7 to 0.0 eV) is enhanced at low coverage relative to the d-band states of the silicide. Although the Pd/Si(100) UPS data do not show clearly any similar behavior, the Si $L_{2,3}$ VV Auger spectrum shows such enhancement [3] for the 94 eV peak, which is derived from states just below E_F . These enhancement phenomena suggest that electronic states specifically associated with the interface may exist in the Si band gap region in addition to the metallic states of the silicide reaction product [3]. Such interface states may be a consequence of the microscopic chemical processes which occur at these reactive interface.

The formation and properties of the refractory metal silicides differ from those for the near-noble metal silicides in significant ways [7], including higher formation temperatures and tendencies for more Si-rich silicide phases and lower Schottky barrier heights on n-Si. UPS result for V/Si(100) are shown in Fig. 3. For 25°C depositions the low-coverage difference spectra show a dominant peak just below E_F ; subsidiary structure (see Figs. 3b and 3c) arises from the attenuation by the metal overlayer of bulk Si emission as well as from the quenching of the intrinsic surface states. At somewhat higher coverage (Fig. 3f) the UPS spectrum shows emission peaked near E_F and limited mostly to the range -4 eV to E_F , as expected for the low energy (occupied) region of the (mostly empty) d-bands of pure V metal; however, further work is required to identify this phase.

The end product of the V/Si reaction [8] is VSi_2 , for which the UPS spectrum is shown in Fig. 3g. This phase was produced by 500°C annealing for a few minutes and was identified by TEM phase analysis. Thus silicide formation may not occur spontaneously at the V/Si(100) interface, but in any case a high interface density-of-states within the Si band gap is produced upon deposition.

Studies like these clearly have the capability to reveal the microscopic chemistry and electronic properties at the metal/Si interface. The existence of well-defined silicide compounds and extensive prior knowledge [8] of aspects of their behavior provides important help in achieving meaningful physical insight from the surface spectroscopic results.

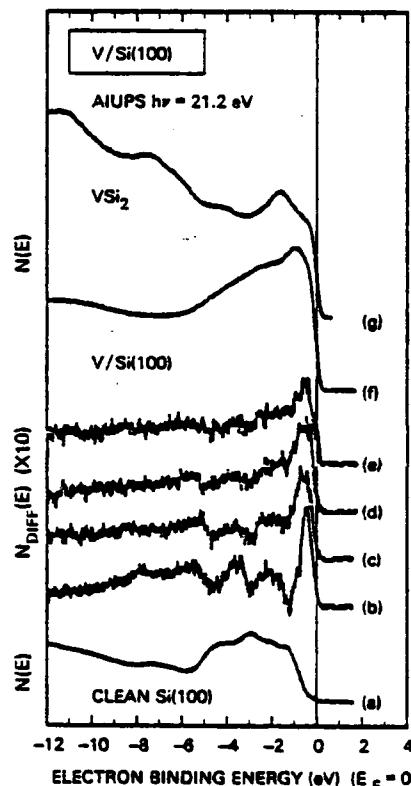


Fig. 3. V/Si(100) results: (a) spectrum for clean Si(100); (b) - (e) incremental difference spectra for V/Si(100), shown in expanded scale for ~ 0.25 - 0.5 Å coverage increments; (f) spectrum for ~10 Å V deposited on Si(100) at 25°C; (g) spectrum for the VSi_2 compound formed by 500°C annealing.

Acknowledgement: VSi_2 phase identification by T.Y. Tan is greatly appreciated, as are discussions with P.S. Ho, J.L. Freeouf, and J. Weaver.

References

*Supported in part by the U.S. Office of Naval Research.

1. J.L. Freeouf, G.W. Rubloff, P.S. Ho, and T.S. Kuan, *Phys. Rev Letters* **43**, 1836 (1979).
2. G.W. Rubloff, P.S. Ho, J.L. Freeouf, and J.E. Lewis, to be published.
3. G.W. Rubloff, P.S. Ho, J.E. Lewis, and J.L. Freeouf, *APS Bulletin* **25**, 266 (1980) and to be published.
4. F.J. Himpsel and D.E. Eastman, *J. Vac. Sci. Technol.* **16**, 1297 (1979).
5. P.S. Ho, G.W. Rubloff, J.E. Lewis, V.L. Moruzzi, and A.R. Williams, submitted to *Phys. Rev.*
6. J.L. Freeouf, *Solid state Commun.* **33**, 1059 (1980).
7. C.A. Crider, J.M. Poate, and J.E. Rowe, *Proc. Symp. on Thin Films and Interfaces, Proc. Vol. 80-2*, p. 135 (The Electrochemical Society, P.O. Box 2071, Princeton, N.J., 1980).
8. See *Thin Films-Interdiffusion and Reactions*, ed. by J.M. Poate, K.N. Tu and J.W. Mayer (Wiley, N.Y., 1978).

CHEMICAL BONDING AND MICROSTRUCTURES OF METAL/SI INTERFACES DURING
SILICIDE FORMATION*

P.S. Ho, H. Föll, J.E. Lewis and P.E. Schmid[†]

IBM, Thomas J. Watson Research Center, Yorktown Heights, N.Y. 10598, U.S.A.

Abstract: Chemical bonding and atomic structure at the $\text{Pd}_2\text{Si}/\text{Si}$ interface have been investigated using Auger electron spectroscopy in conjunction with transmission electron microscopy. Bonding characteristics are derived by interpreting the AES spectra together with UPS spectra based on partial state densities calculated for Pd-Si compounds. Composition calibrations based on Auger intensity variations indicate the existence of enhanced DOS within about 6 Å of the interface which comes mainly from a new 94 eV Si L_{2,3} VV peak in silicide. TEM lattice images show an atomically sharp $\text{Pd}_2\text{Si}/\text{Si}$ interface with misfit dislocations and step-like imperfections present within several atomic layers of the interface. It is suggested that the observed interface states are originated from chemical bonds associated with the interfacial defect structure.

The study of chemical bonding and atomic structure at the metal/semiconductor interface is important for the basic understanding of Schottky barrier formation. Theoretical studies on Schottky barriers have been concerned mostly with interfacial electronic states for nonreacting abrupt interfaces [1]. The interface between a transition metal and Si forms a distinct class by itself because of the strong reactivity which causes formation of silicide compounds at moderate temperatures, e.g. Pd_2Si formed readily at 250°C. [2] During silicide formation, the reaction front proceeds into the Si resulting in a silicide/Si interface with bonding and structural characteristics basically different from those of the non-reacting metal/Si interface. Recently, surface spectroscopy studies [3-7] using UPS, AES and XPS revealed that silicide formation in the first few layers on metal coverage of the Si surface dominates the electronic properties of the Pd/Si, Pt/Si and Ni/Si interfaces. In these studies, very little information has been provided for the correlation between the interfacial atomic structure and chemical bonding although such knowledge is essential for understanding the silicide/Si interface. Here we report results on studying bonding and structure of the $\text{Pd}_2\text{Si}/\text{Si}(111)$ interface using Auger electron spectroscopy in conjunction with transmission electron spectroscopy. The choice of the $\text{Pd}_2\text{Si}/\text{Si}$ system is because that 1. we are interested in the bonding between the Pd d and the Si sp^3 electrons in the silicide and 2. the Pd_2Si basal plane is epitaxial to the Si(111) surface which facilitates the TEM lattice image observations on the interface microstructure.

Experiments were carried out in a UHV chamber equipped with a double-pass CMA for recording the Auger spectra. The Si surface was sputter-cleaned with 1 keV Ar^+ ions then annealed at about 800°C for more than 1/2 hr. to remove the sputter damage. Pd was evaporated at room temperature by in-situ sublimation from a Pd wire and the rate was controlled to provide metal coverage from submonolayer to tens of atomic layers. Beam chopping technique was used to obtain the undifferentiated N(E) spectra directly. After each evaporation, the Si L_{2,3} VV, KLL and Pd M_{4,5} VV Auger spectra were recorded and their relative intensity changes were used to calibrate the silicide composition and thickness.

We describe first briefly the results on chemical bonding of bulk Pd_2Si [8]. In Pd_2Si , the angle-integrated UPS spectra (dominated by the Pd contribution because of its high photoionization cross section) as shown in Fig. 1a indicate that most of the d states become occupied with the major peak B shifted -2.75 eV below E_F . Portion A of the valence states has contributions from both Pd and Si and by being close to E_F , it provides the metallic character for Pd_2Si . The difference in the Si L_{2,3} VV Auger spectra for Pd_2Si and Si as shown in Fig. 1b reflects significant changes in the silicon valence state densities (DOS) as a result of silicide formation which gives rise to a silicide spectrum with four characteristic peaks at 79, 84, 89 and 94 eV.

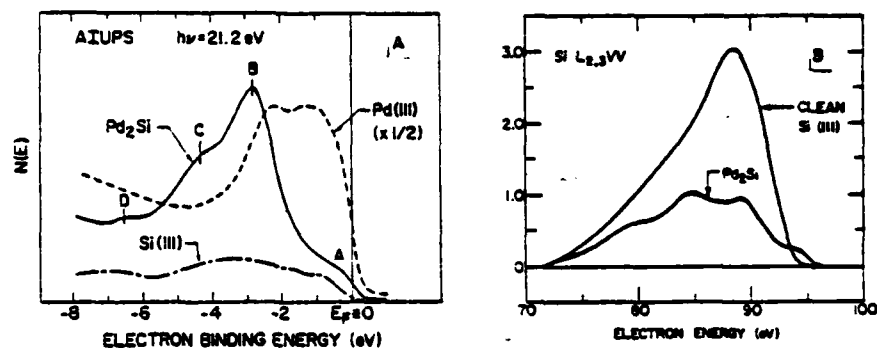


Figure 1. a. Angle-integrated UPS spectra observed on Pd_2Si and on Pd_2Si and on single-crystal Pd(111) and Si(111) surfaces. b. Comparison of the $L_{2,3}VV$ Auger spectra observed on Pd_2Si and Si(111) surfaces.

Chemical bonding information was derived by interpreting the UPS data together with the AES spectra based on partial DOS calculated for Pd-Si compounds. The calculation is self-consistent and based on the Augmented-Spherical-Wave Method [9]. Compounds of the Pd_3Si , PdSi and PdSi_2 stoichiometries in cubic structures of the Cu_3Au , CuAu and CsCl form have been studied. These structures enable us to examine the effect of changing the nearest-neighbor chemical environment on the Pd-Si bond. Results of these calculations show that the total DOS of the compound is dominated by the Pd d states which have features, such as the shift below E_F and the position of the major peak, in qualitative agreement with the UPS results. The Si 3p states form two well defined groups straddling the d band with locations near $E_F (=0)$ and at -5 eV . The Si 3s states lie below the p states at about -10 eV . Schematics for Auger transitions involving the $L_{2,3}(2p)$ level and valence levels from the two p state groups and the 3s states have been worked out [4, 8] which satisfactorily account for the four-peak structure observed in the silicide $L_{2,3}VV$ spectrum. These results lead to the conclusion that the chemical bonding responsible for Pd_2Si formation involves primarily the two 3p groups of Si and part of the Pd d electrons. The hybridization of these p and d electrons forms the basic bonding and anti-bonding states in Pd_2Si .

Pertinent to the interfacial electronic structure are the spectroscopy results observed during in-situ evaporation of Pd layers. UPS results [3,10] revealed that the valence spectra associated with the interface have the characteristic form of the silicide accompanied with shifts of the major peak B from -3.5 eV at low coverage to -2.75 eV at about 12\AA coverage. The $L_{2,3}VV$ Auger spectra observed for increasing coverages are shown in Fig. 2a. To discern changes caused by interface reaction, we decompose each spectrum into two parts, one has the elemental Si form and the remain gives the changes due to silicide formation; only the latter is shown in Fig. 2b. Here two points are worth noting. First, the intensity of the 94 eV peak reaches a maximum at about 7\AA coverage while the rest of the intensity increases with further coverage; and second, the 94 eV peak shifts toward lower energies with coverage, maximizing at about 1 eV shift for Pd_2Si . The calculated DOS reveals that stoichiometry increase of Si in the compound shifts the position of the d peak toward lower energies as well as increases the occupation of the antibonding 3p states near E_F . This is consistent with the UPS results; in addition, by noting that the 94 eV peak involves two antibonding p states, the calculated DOS also explains the changes in position and energy of this Auger peak. Thus it appears that stoichiometry gradient with Si enrichment near the interface can account for the spectroscopy results. Indeed, it has been proposed that an interfacial silicide of the MSi_4 stoichiometry can be used as a basis to confirm the Schottky model for silicide/Si interface. [11]

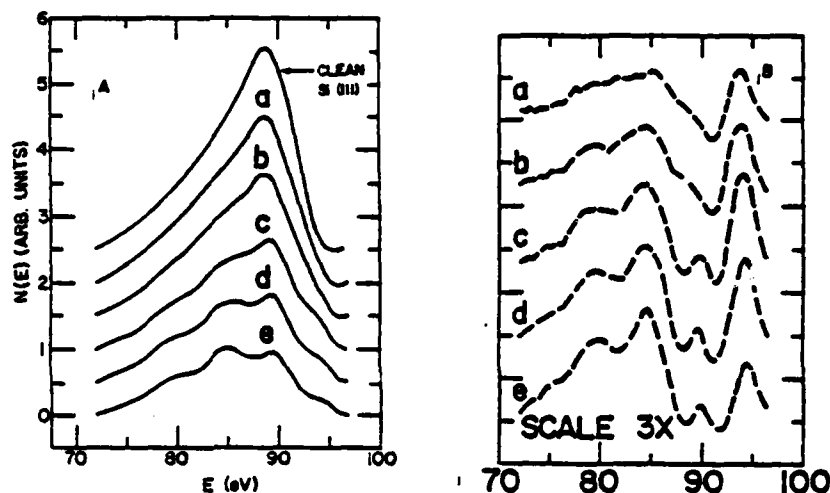


Figure 2. a. The Si $L_{2,3}$ VV Auger spectra observed at the Pd/Si(111) interface as a function of Pd coverage. Pd thickness: a. 1 Å, b. 3 Å, c. 10 Å, d. 17 Å, e. 30 Å. b. The $L_{2,3}$ VV spectra in a are decomposed by subtracting off the elemental Si spectrum. Here the difference shows features mainly associated with interfacial silicide formation.

Several relevant issues concerning the interface stoichiometry gradient have to be resolved. First, since TEM observations show only the Pd_2Si phase existing in the reactive Pd/Si interface, it is difficult to justify thermodynamically a large stoichiometry variation in one phase. Second, there is no direct stoichiometry measurement within, e.g. 10 Å of the interface, to confirm the Si enrichment of the compound. And third, since the electron spectroscopy senses only the localized atomic environment, it does not provide information on the overall atomic structure for the interface. To investigate these problems, we used the cross-sectional TEM to examine the interfacial structure and Auger intensity calibration to determine the composition of the interface layer.

In Fig. 3a we show the TEM lattice image of the Pd_2Si /Si(111) interface as obtained from a sample where Pd_2Si was formed by evaporating ~ 100 Å of Pd on a chemically clean Si surface. In Si the image shows the {111} and {220} planes which are interwoven to yield the <110> channels while in Pd_2Si , the {2240} planes are observed. These lattice images clearly extend to the interface indicating that an atomically sharp Pd_2Si /Si interface exists with no amorphous-like structure. It is significant, however, to point out the two types of structural imperfections at the interface. One is the misfit dislocations which can be detected by counting the differences in the numbers of lattice fringes on the two sides of the interface and the other are steps ranging from monolayer to several atomic layers. As illustrated in Fig. 3b, both types of defects are able to change the local bonding configuration without varying the overall lattice structure. In addition, even for an ideal interface, the abrupt termination of the crystals at the interface produces bonds with unique interfacial character. These results demonstrate that bonds distinct from those in bulk Pd_2Si exist at the Pd_2Si /Si interface to a depth of several atomic layers.

The composition calibration is based on the relative intensity variations of the Si LVV and KLL vs the Pd MVV lines. The depth sensitivity of the calibration comes from the different escape distances of these Auger lines. Based on the shape difference, one can separate the elemental Si from the silicide contribution to the LVV intensity, thus the intensity variation of the silicide DOS can be examined within the escape distance of the LVV electrons (about 7 Å) from the interface. Calibrations of data from several runs similar to that shown in Fig. 2 reveal that while the combination of the elemental Si LVV, Pd MVV and Si KLL intensities shows formation of the same silicide

extending to the interface, extra Si DOS associated with the silicide (primarily from the 94 eV peak) are clearly observed within about 6 Å from the interface.

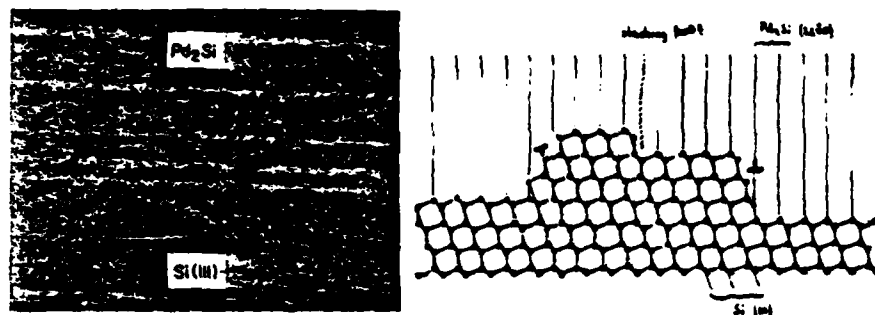


Figure 3. a. TEM lattice image observed in a vertical cross section of the $\text{Pd}_2\text{Si}/\text{Si}$ interface. b. Schematic illustration of structural imperfections of steps and misfit dislocations.

The calibration results alone is insufficient to resolve the question whether the extra DOS is caused by interfacial states or by a stoichiometry gradient near the interface. However, when they are combined with the structural information, particularly noting that the atomic roughness of the interface is consistent with the range of the extra Si DOS, we are led to believe the answer to be the existence of Si interface states at the $\text{Pd}_2\text{Si}/\text{Si}$ interface, which seem to be originated from structural imperfections, e.g. steps and misfit dislocations. The fact that the extra intensity comes from the 94 eV peak further suggests that the interface states are associated with the antibonding states of $\text{Pd}(4d)\text{-Si}(3p)$ hybrids near E_F . Details concerning the nature of the structure and bonding of the interface states are being studied.

*Work supported in part by the office of Naval Research

†Supported in part by the Swiss National Research Foundation

1. See, for example, papers in *J. Vac. Sci. Technol.* 935-1028 (1974).
2. K.N. Tu and J.W. Mayer, Chap. 10 in *Thin Film - Interdiffusion and Reactions*, ed. by J.M. Poate, K.N. Tu and J.W. Mayer (Wiley, New York, 1979).
3. J.L. Freeouf, G.W. Rubloff, P.S. Ho and T.S. Kuan, *Phys. Rev. Letters* 43, 1836 (1979).
4. J.A. Roth and C.R. Crowell, *J. Vac. Sci. Technol.* 15, 1317 (1978); also J.A. Roth, Ph.D. Dissertation, Univ. of Southern Calif. (June 1979).
5. P.S. Ho, T.Y. Tan, J.E. Lewis and G.W. Rubloff, *J. Vac. Sci. Technol.* 16, 1120 (1979).
6. P.J. Grunthaner, F.J. Grunthaner and J.W. Mayer to be published.
7. J.N. Miller, S.A. Schwarz, B. De Michelis and I. Abbati, to be published.
8. P.S. Ho, G.W. Rubloff, J.E. Lewis, V.L. Moruzzi and A.R. Williams.
9. A.R. Williams, D.D. Gelatt Jr. and V.L. Moruzzi, *Phys. Rev. Lett.* 44, 429 (1980).
10. G.W. Rubloff, P.S. Ho, J.L. Freeouf and J.E. Lewis, to be published.
11. J.L. Freeouf, *Solid State Commun.* 33, 1059 (1980).

RC 8165 (#35495) 3/18/80
Surface Science 10 pages

CHEMICAL BONDING AND ELECTRONIC STRUCTURE OF Pd_2Si

P.S. Ho, G.W. Rubloff, J.E. Lewis, V.L. Moruzzi and A.R. Williams

IBM Thomas J. Watson Research Center
Yorktown Heights, New York 10598

Typed by: Lorraine Miro

ABSTRACT: The chemical bonding and electronic properties of Pd_2Si have been investigated by measuring UPS and AES transitions involving both core and valence electrons for Pd, Si, and Pd_2Si . The spectra have been interpreted based on partial state densities calculated for Pd-Si compounds. In the silicide, the d states of the Pd interact strongly with the p states of the Si. The resulting p-d hybrid complex is composed of Pd d states lying almost entirely below E_F with the central peak at -2.75 eV and two groups of Si states separated by ~5 eV. The lower-lying group of Si states forms the Si(3p)-Pd(4d) bonding levels while the higher-lying group near E_F forms the corresponding anti-bonding states. The compound stoichiometry can change the position of the d peak as well as the occupation of the antibonding states, thus affecting the phase stability of the compound. Such stoichiometry variations are consistent with a rigid band filling of the d-p complex. The results obtained in this study can be used to account for the transport properties of Pd_2Si .

To be published in Phys. Rev. B15 (Nov. 1980).

I. INTRODUCTION

The formation of silicide compounds at metal/Si interfaces is of current interest because of the potential device applications and the need for basic understanding of the properties of metal-semiconductor interfaces. Extensive studies have been carried out on the material properties of silicides¹, such as phase identifications and formation kinetics; however, the electronic or chemical bonding characteristics of these compounds have not been systematically investigated. Knowledge of the electronic properties of the silicide and at the interface is important for understanding the formation mechanism of Schottky barriers and Ohmic contacts at silicide/Si interfaces. In this regard, it is relevant to distinguish interfaces where metal-Si compounds can be formed e.g. Pd/Si and Pt/Si, from those where such compounds do not exist e.g. Al/Si and Au/Si. The formation of a specific compound defines the local atomic and chemical environment in the silicide lattice and to a significant extent at the silicide/Si interface as well, whereby the electronic properties are largely determined. In contrast, most of the properties of the nonreacting interface may be characteristic of the discrete nature of the ideal metal/Si interface, e.g. metal-induced gap states.² In addition, compound formation proceeds at a reaction interface which is created continuously by atomic rearrangement resulting from material reactions. This tends to better preserve the intrinsic characteristics of the interface since it is less susceptible to interfacial contamination effects than are the noncompound-forming interfaces. Indeed, we reported earlier in a study of the Pd/Si interface³ that microscopic compound formation dominates the chemical and electronic properties of the Pd/Si interfaces.

We have completed a study of silicide formation at the Pd/Si interface using ultraviolet photoemission spectroscopy (UPS) and Auger electron spectroscopy (AES). The reason for choosing the Pd/Si system is three-fold. First, we wish to explore the nature of the chemical bonding between the metal d and the Si s-p electrons underlying the mechanism for transition-metal silicide formation. Second, the basal plane of Pd₂Si and the Si(111) surface have an epitaxial relationship with less than 2% lattice misfit⁴, so the atomic structure of the interface is expected to be simple. Third, extensive data on silicide formation in the Pd/Si system show formation of only one compound, Pd₂Si, and that is stable up to 700°C but can still be readily formed at 200°C.⁵ The compound stability and fast reaction kinetics suggest a strong chemical interaction between the Pd and Si atoms. All these factors facilitate our prototype study of the metal/Si interface.

Results of our study are reported in two papers. Here, the first one describes results for bulk Pd₂Si formed by reacting relatively thick (~100Å)

Pd overlayers with Si. The chemical bond and electronic characteristics of the compound are inferred by interpreting the spectroscopy data using calculated electronic density of states (DOS) for Pd, Si, and Pd-Si compounds. The sequel paper deals with the chemical bonding and reactions at the Pd/Si interface observed during the initial stage of silicide formation.

II. EXPERIMENTAL

All experiments were carried out on single-crystal Si substrates of 1 to 10 Ω -cm resistivity. Before Pd evaporation, the Si substrate was sputter-cleaned using Ar^+ ions of 1 keV energy and then annealed by direct resistive heating up to about 850°C for about 10 min. to remove the sputter damage. LEED examination of some sample surfaces showed the annealing procedure to be sufficient to produce the reconstructed (7x7) Si(111) surface or a (1x1) Si(111) surface (probably a disordered (7x7) structure). Observations by transmission electron microscopy (TEM) revealed that the Pd_2Si formed on the (111) Si substrates after sputtering and annealing treatments was not epitaxial in all areas, indicating incomplete recovery of the surface sputter damage.⁶ However, the features of the UPS and the AES spectra were independent of the degree of epitaxy of the Pd_2Si .

Pd evaporations were made by direct sublimation of a resistively heated Pd wire (0.25 mm. dia.) in the ultrahigh vacuum chamber. During evaporation, the pressure rise was less than 2×10^{-9} torr. Auger examination of the Pd surface usually revealed no detectable surface contaminants (i.e., less than 1% surface coverage). Pd thickness was measured by a thickness monitor (for UPS measurements) or calibrated according to the relative intensity changes of the Pd and Si Auger lines with different electron escape distances.⁷ Data reported here were all obtained on samples with Pd thickness more than about 50Å. For these samples, the conversion of Pd into Pd_2Si was carried out by annealing at about 200°C where a few minutes were sufficient for a complete conversion (as confirmed by TEM phase identification).

Spectroscopy data were taken using a double-pass cylindrical mirror analyzer with an energy band pass of 0.6%. UPS measurement used a differentially pumped He resonance lamp for photon excitation ($h\nu=21.2$ eV) and electron counting techniques. For AES measurements, the electron gun was operated at 5 keV and a beam chopping method was used to obtain the undifferentiated $N(E)$ spectra directly. Measurements were made on the Pd $M_{4,5}$ VV and Si $L_{2,3}$ VV and KLL Auger transitions. The first two valence state transitions were used to monitor changes in the valence electronic structure of Pd and Si a result of silicide formation. There are two other Si valence transitions, the LLV and the KLV lines, which are simpler to interpret since only one valence level is involved.

They were not used because of the LLV energy overlap with Pd lines and the weak intensity of the KLV line. The core KLL transition was used mainly to obtain the relative changes in the Auger line intensities in order to determine the composition and thickness of the silicide layer. Here it suffices to mention that the results presented in this paper were obtained from samples which have been identified by Auger composition calibration and TEM diffraction techniques to be the Pd_2Si compound.

III. RESULTS

a. Photoemission and Auger Spectroscopy

In Fig. 1 the angle-integrated UPS spectrum of Pd_2Si formed on Si(111) is compared with spectra from clean single-crystal Pd(111) and Si(111) surfaces. The considerably larger intensity in the Pd(111) and Pd_2Si spectra arises from the large Pd 4d photoionization cross section, which causes the Pd_2Si spectrum to be dominated by the Pd d states. Comparing the Pd(111) and Pd_2Si spectra, the 4d band is seen to be shifted toward lower energies as a result of silicide formation; the main Pd_2Si peak B appears about -2.75 eV below the Fermi level E_F . The width of the d band is not greatly changed but those empty d states in Pd metal (above E_F) now become essentially completely filled. These features indicate an electronic structure for Pd in the silicide more like that of the noble metals than the transition metals. The formation of Pd_2Si also brings forth new, but relatively weak, peaks at C and D. In addition, electronic states exist near E_F which produce a characteristic Fermi level cutoff shape at E_F . This portion of the DOS (designated as A) gives a metallic character for Pd_2Si . The detailed nature of the electronic states contributing to these structures cannot be readily assessed on the basis of the UPS data alone although it is expected that they involve not only the Pd but also the Si valence states. This will be discussed later in conjunction with results from AES measurements and band calculations.

In Fig. 2a we compare the Si $L_{2,3}\text{VV}$ spectrum for elemental Si with that in Pd_2Si . It is clear that the formation of the silicide significantly alters the line shape of the LVV transition, thus reflecting basic changes in the valence structure of Si. For clarity, we decompose the silicide LVV spectrum into two portions as shown in Fig. 2b with one portion scaled according to the LVV shape of elemental Si and the other showing the change in the spectrum. The silicide spectrum displays peaks at 79, 84, 89 and 94 eV. The origin of these peaks will be discussed later; at this point, it is interesting to note that these peaks are separated by about 5 eV energy differences.

In contrast, the KLL Si line for Pd_2Si as shown in Fig. 3 exhibits little change from that of elemental Si. This leads to the obvious conclusion that the formation of silicide changes primarily the valence states of Si but does not change its core level positions greatly (<1 eV.) In Fig. 4, the $\text{M}_{4,5}\text{VV}$ spectra for Pd obtained from a pure Pd film and from Pd_2Si are shown. The shape of the main doublet in the spectrum shows no visible difference as a result of silicide formation. The lower energy peak A of this spectrum comes from transitions involving $3d_{5/2}$ core states and the higher energy one (B) corresponds to transitions involving the $3d_{3/2}$ states. The separation of these two 3d peaks caused by spin-orbit splitting is about 5 eV in pure Pd as determined by XPS measurements.⁸ The $\text{M}_{4,5}\text{VV}$ Auger transition has an energy separation between A and B still of 5 eV, so the relative levels of the two 3d states do not change upon the formation of silicide and its line width of about 10 eV reflects the transition arising from self-convolution of the 4d valence states (5 eV wide). These features agree quantitatively with the results obtained in a similar spectroscopic study on amorphous Pd-Si metallic glasses.⁸ In the amorphous compound study, the high energy peak of the compound was observed to shift about 1 eV toward lower energy. This magnitude of energy shift cannot be ascertained in our measurements. In our Pd_2Si spectrum, a new peak appears at about 302 eV. The intensity of this peak was observed to increase with Pd layer thickness during the initial stage of silicide formation so it is associated with silicide formation. The origin of this peak is not clear at present.

b. Calculated State Densities

The UPS and AES results indicate significant changes in the valence electronic structures of both Pd and Si upon silicide formation. Extracting information relevant to the bonding characteristics requires lineshape analysis of the spectra which is not straightforward. As noted earlier, although the UPS spectrum is dominated by Pd 4d contributions, Si contributions are also present, so that a distinction between these two cannot be made by UPS data alone. The Auger spectrum is specific to the local Si or Pd electronic structure but it involves a self-convolution of the valence state densities; the multi-state nature of the transition makes it difficult to deconvolute the valence density of states.

To facilitate the interpretation of the measured spectra, calculations of density of state were carried out for both Pd, Si and several Pd-Si compounds (although here we will only show results of two compounds most relevant to our data interpretation). To describe the crystal structure used in the calculation, it is useful to examine first the lattice structure of Pd_2Si . This compound has a hcp structure with atomic arrangements for the two basic stacking layers⁴ as shown in Fig. 5. The structure shows that each Si atom is encased by 9 Pd atoms stacking in 3 equi-lateral triangles with 60°

relative rotations. Probably the most important aspect of this structure in affecting the Si spectra is that the tetrahedral environment of elemental Si is completely eliminated; each Si is completely surrounded by Pd atoms. Limitations of our computer programs prevent us from studying Pd_2Si in the hexagonal structure. However, our self-consistent calculations for Pd/Si compounds in the Cu_3Au , CuAu and CsCl structures reveal, we feel, the important properties of the Pd/Si bond, such as the role of stoichiometry, the importance of charge transfer, the strength of the bond and the implications of depriving the Si atoms of the Si neighbors. In Fig. 5b we show the CuAu and Cu_3Au type crystal structure for Pd_3Si and PdSi . All three of the structures used in the calculations permit the Si atoms to be surrounded by Pd atoms. Furthermore, comparison of the results for the CsCl and CuAu structures provides an indication of the importance of the local geometrical structure. In all cases total-energy minimization was used to determine the lattice constant and to assess the bonding strength.

The calculations employ the Augmented-Spherical-Wave method.⁹ The aspects of this method which are important in the present context are: (1) it is fully self-consistent (if charge transfer were important, we would see it.); (2) calculated heats of formations agree well with experiment^(9,10); and (3) the only input to these calculations is the atomic numbers of the constituents and the crystal structure.

Figures 6 and 7 show the calculated DOS for PdSi and Pd_3Si in the CuAu and Cu_3Au structures (fcc-like). Also shown are the partial (projected) DOS corresponding to the Si and Pd sites. Several aspects of the state densities should be noted. First, the total state densities for PdSi and Pd_3Si are qualitatively similar, indicating that rigid-band theory is the appropriate perspective from which to consider stoichiometry changes. The principal difference between PdSi and Pd_3Si is the position of the Fermi level. Second, the d states of the Pd dominate the total state density. One should note, however, that the DOS near E_F (position A) is not exclusively due to the d states; rather the Si 3p states contribute about equally, and a similar situation exists in the tail portion (D) of the d band at about 5.5 eV below E_F . Third, the density of Si p states indicates two well defined groups of states which straddle the d band. These two groups reflect the formation of bonding and anti-bonding $\text{Si}(3p)\text{-Pd}(4d)$ hybrids. The chemical bond in Pd_2Si does not seem to involve the Si 3s states since most of them remain about 10 eV below E_F . The large effect on the Si 3p states is not unexpected since these states are mainly responsible for the directionality in the covalent bond of Si, which is completely absent in the silicide.

IV DISCUSSION

In studying the UPS spectrum of amorphous PdSi compounds, Riley et al.⁸ estimated the cross section ratio $\sigma(\text{Si } 3p)/\sigma(\text{Pd } 4d)$ to be about unity. Judging from this ratio and the relative numbers of valence electrons for Pd and Si (20 vs. 4 in Pd_2Si), the UPS spectrum for Pd_2Si is expected to reflect rather closely the total DOS with dominant contributions from the Pd d states. On this basis the UPS data and the calculated DOS are in good agreement, with both showing the Pd d band being completely occupied and the major d peak shifted to about -2.75 eV below E_F . Interestingly, the shift of the major d peak was not constant but rather was observed to vary from -3.5 eV at submonolayer Pd coverage to -2.75 eV in bulk Pd_2Si .³ This shift and the stoichiometry dependence of the d peak/Fermi level separation (larger for higher Si concentration) seen in the calculated DOS (Figs. 6 and 7) suggest that early stages of the interface are Si-rich as compared to Pd_2Si . The implication of such stoichiometry effects on the interface properties will be discussed in the sequel paper.

The energy-band calculations indicate that the principal factor in the d peak displacement is not charge transfer, but rather the formation of a hybrid complex resulting from the strong interaction of the p(Si) and d(Pd) states. The d component of this complex, while well defined in the photoemission spectrum, contains sufficiently fewer than ten electrons that its position below E_F does not imply significant charge transfer.

For AES, Sawatzky¹¹ showed that for transitions involving two valence states, the spectrum is quasi-atomic if the Coulomb interaction between the two holes is much larger than the bandwidth; otherwise it resembles the self-convolution of the DOS of the valence band. Previous Auger studies^{12,13} on d metals showed that the quasi-atomic character holds in general for the $M_{4,5}VV$ transitions. Since the observed $M_{4,5}VV$ line shape was almost identical for Pd and Pd_2Si we infer that the Pd local charge density remains quasi-atomic in the silicide lattice. This is really not surprising since the local Pd configuration in Pd_2Si is primarily of the nearest-neighbor Pd-Pd type.

Riley et al.⁽⁸⁾ have also concluded from the peak shift of the Pd $M_{4,5}VV$ line that negligible charge transfer occurs between Pd and Si in the amorphous Pd-Si metallic glass. This is consistent with our observation of the Pd $M_{4,5}VV$ transition in Pd_2Si as well as with our calculated state densities.

In contrast, the Si $L_{2,3}VV$ transition satisfies the band-convolution criterion and the lineshape of this transition has been investigated and successfully understood for elemental Si in a number of theoretical studies.¹⁴⁻¹⁶ The conclusion generally reached is that the spectrum is dominated by the p-p type transitions involving two 3p valence states,

which account for most of the intensity for the 89 eV peak. As for the other transitions, the s-p types represent only about 10%, contributing mainly to the tail portion of the spectrum, and the s-s transitions are negligibly small. These weightings are attributed to matrix element effects¹⁴ which suppress contributions from the overlap (bonding) charge density of the s-like atomic orbitals.

For Pd_2Si , the observed $L_{2,3}\text{VV}$ spectrum can be qualitatively understood based on the Si DOS obtained from our calculations and schematics for the Si $L_{2,3}\text{VV}$ transitions in the silicide are shown in Fig. 2c. The 5 eV splitting of the bonding (p_b) and antibonding (p_a) states can account for peaks at 94 eV (p_a-p_a), 89 eV (p_b-p_a) and 84 eV (p_b-p_b). Additionally, transitions involving the p_a , p_b and 3s states contribute to the peaks at 79 eV and 84 eV respectively. Evaluation of the lineshape would require detailed calculation of the silicide spectrum which is presently under study¹⁷; however, Roth¹⁸ has recently derived the Si valence DOS by self-deconvolution of the $L_{2,3}\text{VV}$ spectrum observed for Pd_2Si , and his results agree generally with our schematics of the transitions.

We found that the 94 eV peak was more readily observed at low Pd coverages than the 79 and 84 eV peaks, with its intensity reaching a relative maximum under about two monolayers ($\sim 3\text{\AA}$) of Pd coverage. This reveals enhanced DOS existing in the band gap during the initial stage of silicide formation. (Details of this observation and its stoichiometry dependence will be discussed in the sequel paper). Since the 94 eV peak originates from the p_a antibonding states which are mostly empty in Pd_2Si , we speculate that the antibonding states contribute to the Si $L_{2,3}\text{VV}$ Auger spectrum because they are the states constituting the screening charge brought to the Si site by the core hole responsible for the Auger transitions. (The initial state from the viewpoint of the Auger transitions is the fully screened final state of the core-hole-creation process.^{19,20})

Summarizing the AES and UPS results, the formation of Pd_2Si is found to affect both the Pd- and Si- derived states: for Pd, the d states become "filled" and shifted to about -2.75 eV below E_F ; for Si, the 3p states are split into two peaks of about 5 eV apart, while the 3s states remain about 10 eV below E_F and not much affected. The chemical reactions responsible for Pd_2Si formation involve Pd(4d) - Si(3p) bonding states at about -5.5 eV and antibonding states near E_F . These overall features of the chemical bond for Pd_2Si crystalline compound are quite similar to those observed for amorphous $\text{Pd}_{81}\text{Si}_{19}$ metallic glass.⁸ The calculations demonstrate that stoichiometry can affect compound stability by varying the occupation of the antibonding states. This is also reflected in the calculated heat of formation which shows a sharp variation with the stoichiometry. All these results indicate that the stable stoichiometry is determined by the

energy benefit of positioning E_F below the antibonding state, so the silicide in the Pd-Si system tends to contain more Pd than the 50:50 ratio in order to improve its phase stability.

Finally the electronic structure of Pd_2Si as deduced here can be used to account for its transport properties. Wittmer et al²¹ measured the transport properties of Pd_2Si from the Hall mobility and the electrical conductivity. They concluded that Pd_2Si is metallic with negative charge carriers of average mobility but were unable to explain the low conductivity value which amounts to only about $\frac{1}{6}$ of the mobile charges. We have already pointed out the metallic character of Pd_2Si . Significantly, our results show also that most of the d band is shifted about 2 to 3 eV below E_F so these d electrons do not contribute to the transport properties, thus the mobile charges come only from the small portion of the total electrons located near E_F as observed by these authors. Interestingly, these electrons are also responsible for part of the chemical bond between Pd and Si atoms in Pd_2Si .

ACKNOWLEDGEMENT

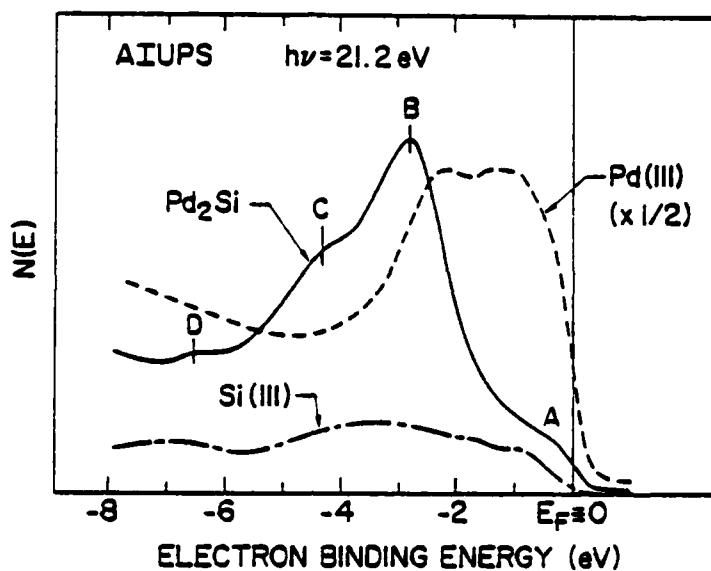
We wish to thank Drs. K. N. Tu and J. L. Freeouf for valuable discussions during the course of this work and Dr. T. Y. Tan for his TEM phase identification of the Pd_2Si .

*This work was supported by the Office of Naval Research.

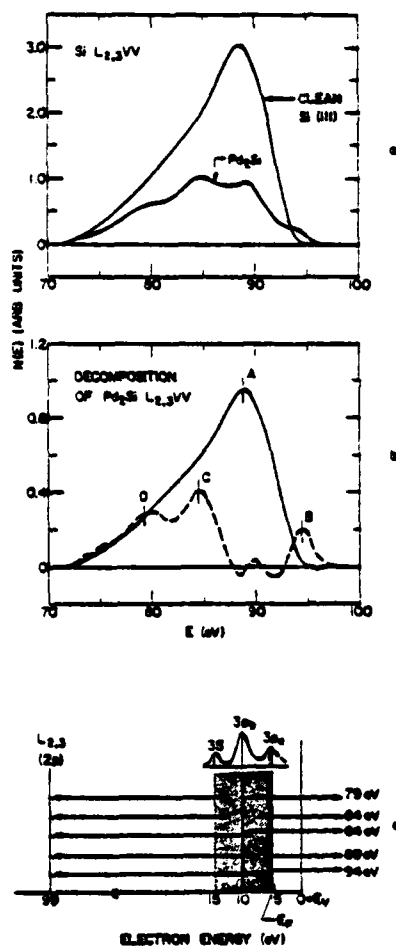
REFERENCES

1. K.N. Tu and J.W. Mayer in "Thin Films-Interdiffusion and Reactions", ed. by J.M. Poate, K.N. Tu and J.W. Mayer, John Wiley, New York (1978), Chp. 10, p.359.
2. See, for example, G. Margaritondo, J.E. Rowe and S.B. Christman, Phys. Rev. B14, 5396 (1976).
3. J.L. Freeouf, G.W. Rubloff, P.S. Ho and T.S. Kuan, Phys. Rev. Lett. 43, 1836, (1979).
4. W.D. Buckley and S.C. Moss, Solid-State Electron., 15, 1331 (1972).
5. C.J. Kircher, Solid State Electron., 14, 507 (1971); D. Sigurd, W. van der Weg, R. Bower and J.W. Mayer, Thin Solid Films, 19, 319 (1974).

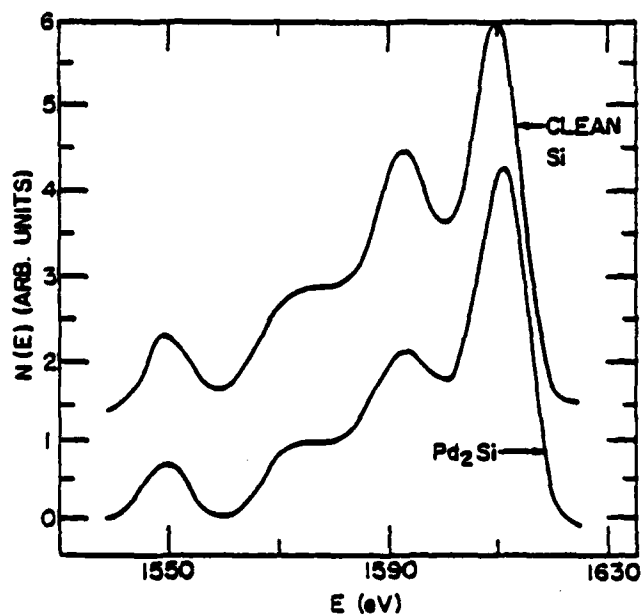
6. T.Y. Tan, private communication.
7. P.S. Ho, T.Y. Tan, J.E. Lewis and G.W. Rubloff, J. Vac. Sci. Technol. *16*, 1120 (1979).
8. J.D. Riley, L. Ley and J. Azoulay, Phys. Rev. *B20*, 776 (1979).
9. A.R. Williams, J. Kubler and C.D. Gelatt, Jr., Phys. Rev. *B19*, 6094 (1979).
10. A.R. Williams, C.D. Gelatt Jr. and V.L. Moruzzi, Phys. Rev. Lett. *44*, 429 (1980).
11. G.A. Sawatzky, Phys. Rev. Lett. *39*, 504 (1977).
12. J.M. Mariot and G. Dufour, J. Elect. Spect. and Related Phenom. *13*, 403 (1978).
13. A.C. Parry-Jones, P. Weightman and P.T. Andrews, J. Phys. C: Solid State Phys. *12*, 1587 (1979).
14. J.E. Houston, M.G. Lagally and G. Moore, Solid State Commun. *21*, 879 (1977).
15. P.J. Feibelman, E.J. McGuire and K.C. Pandey, Phys. Rev. *B15*, 2202 (1977); P.J. Feibelman and E.J. McGuire, Phys. Rev. *B17*, 690 (1978).
16. D.R. Jennison, Phys. Rev. *B18*, 6865 (1978).
17. K.C. Pandey, private communication.
18. J.A. Roth, Ph.D. Dissertation, Univ. of Southern Calif. (June 1979).
19. N.D. Lang and A.R. Williams, Phys. Rev. *B16*, 2408 (1977).
20. A.R. Williams and N.D. Lang, Phys. Rev. Lett. *40*, 954 (1978).
21. M. Wittmer, D.L. Smith, P.W. Lew and M.A. Nicolet, Solid State Commun. *21*, 573 (1978).



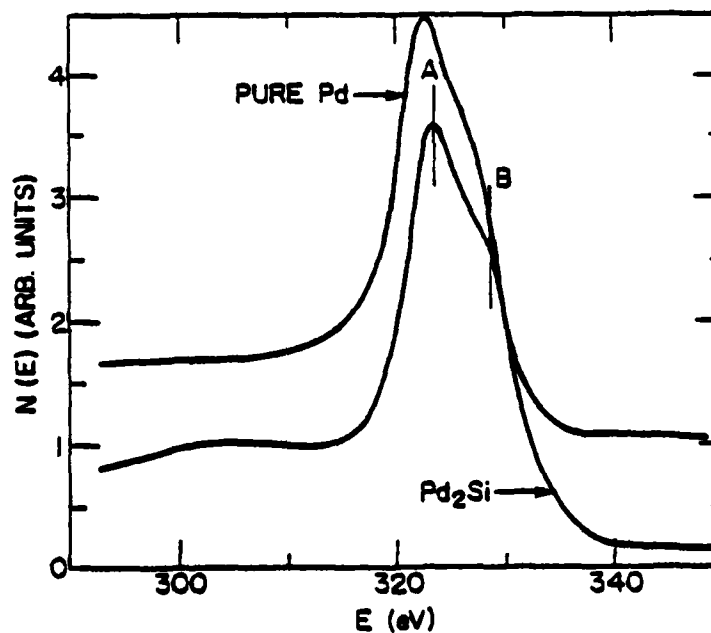
1. Angle-integrated UPS spectra observed on Pd_2Si and on single-crystal Pd(111) and Si(111) surfaces. Note the difference in the intensity scales revealing the dominance of the Pd 4d states in the Pd_2Si spectrum.



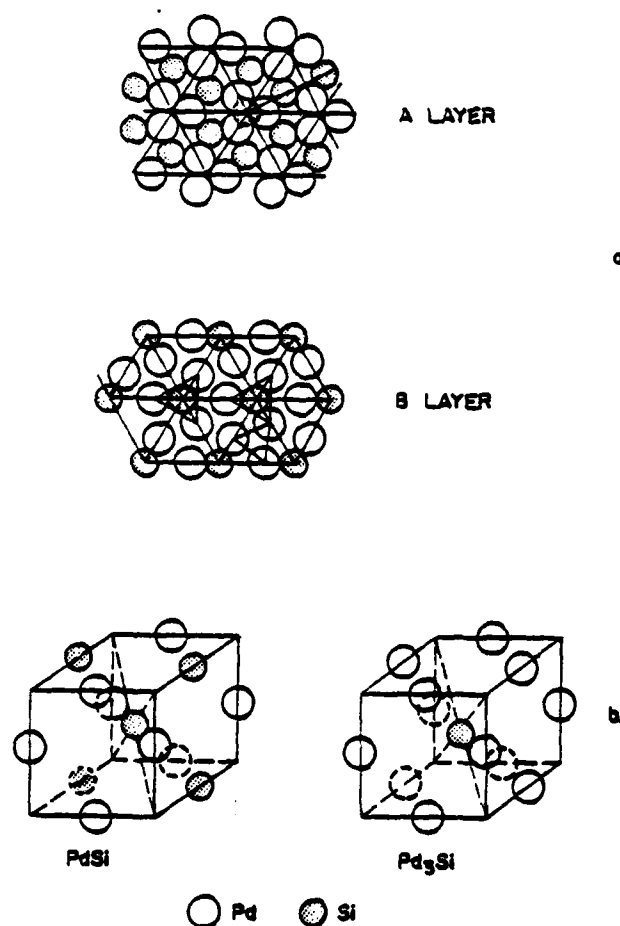
2. a. Comparison of the $L_{2,3}VV$ Auger spectra observed on Pd_2Si and $Si(111)$ surfaces. b. Decomposition of the Auger spectra into two portions with the solid line portion proportional to the elemental peak and the dash-line portion showing the change as a result of silicide formation. c. Schematics of the Auger transitions for Si $L_{2,3}VV$ in Pd_2Si according to calculated state densities.



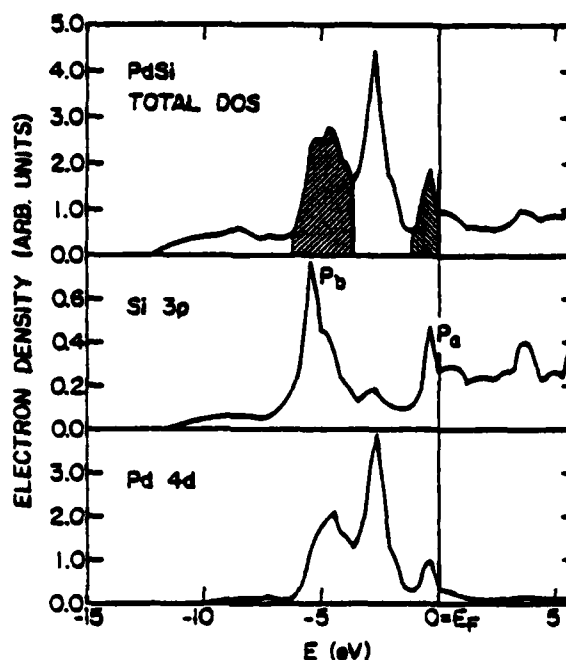
3. Comparison of the Si KLL spectra observed on Si(111) and Pd_2Si surfaces. (Intensities normalized for the main peak).



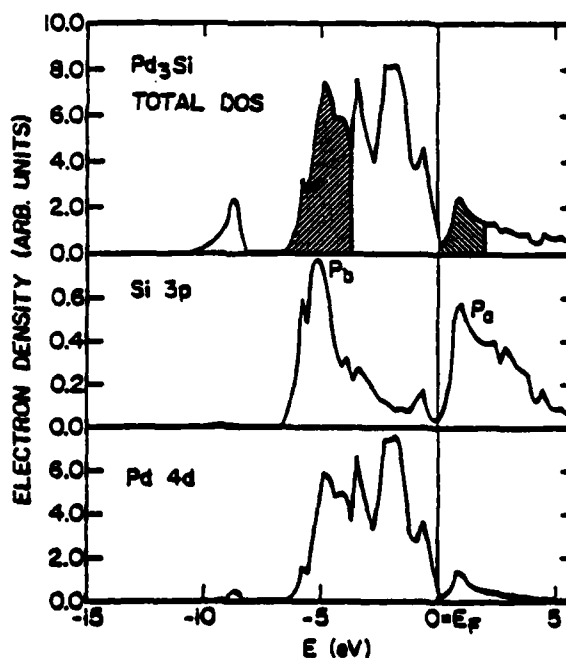
4. Comparison of the Pd $M_{4,5}VV$ Auger spectra observed on a polycrystalline Pd surface and a Pd_2Si surface formed on Si(111) substrate. (Intensities normalized for the main peak.)



5. a. Atomic arrangements on the two basic layers forming Pd₂Si structure. The hcp Pd₂Si structure has a stacking sequence of ABAB. b. The CuAu and Cu₃Au type crystal structures of PdSi and Pd₃Si used for calculating DOS of Pd-Si compounds.



6. Calculated total and partial state densities for Pd, Si and PdSi compound. Note the difference in the vertical scales for the state densities. The shaded areas in the total DOS indicate the bonding and antibonding states.



7. Calculated total and partial state densities for Pd, Si and Pd₃Si compound. Note the difference in the vertical scales for the state densities. The shaded areas in the total DOS indicate the bonding and antibonding states.

RC 8437 (#36721) 8/27/80
Surface Science 29 pages

CHEMICAL BONDING AND REACTIONS AT THE Pd/Si INTERFACE*

G. W. Rubloff, P. S. Ho, J. L. Freeouf, and J. E. Lewis

IBM Thomas J. Watson Research Center
Yorktown Heights, New York 10598

Typed by Janis T. Riznychok (GR.2511)

Abstract

The electronic structure of the clean Pd/Si(111) and Pd/Si(100) interfaces has been investigated using angle-integrated and angle-resolved ultraviolet photoemission (UPS) and Auger electron spectroscopies (AES), in conjunction with TEM, work function, and LEED measurements. Since the interface is highly reactive, studies were made by processing the reaction in two ways: (i) sequential annealing steps of thick metal overlayers, and (ii) sequential deposition steps of very thin metal overlayers (considerably less than a monolayer per step). The UPS and AES spectra of the bulk reaction product (Pd_2Si) were first determined in films sufficiently thick for TEM phase analysis ($\geq 5\text{\AA}$), taking care to be sure that surface segregation effects (due to thin film reaction kinetics) in these cases were negligible. On this basis, lower coverage (submonolayer) spectra could then be interpreted. Formation of the Pd_2Si compound is interface-driven and extremely rapid at the clean Pd/Si interface. This compound formation dominates the microscopic chemistry and electronic properties of the interface. Chemical shifts observed in the electron spectroscopy measurements can be interpreted in terms of stoichiometry variations in the Pd_2Si compound (i.e. retaining its lattice structure); these appear as Si-rich Pd_2Si near the interface, with the Si excess decreasing with distance from the interface. Although silicide formation accounts for most aspects of the electronic structure, other effects such as localized interface bonds, defect states, etc. may make additional contributions at low metal coverage.

Submitted to Phys. Rev. B15.

Introduction

Chemical bonding (i.e. electronic structure coupled with atomic microstructure) determines many of the properties of the metal/semiconductor interface. Because of its significance in semiconductor device applications, the most important electrical property is probably the Schottky barrier height: ohmic (low barrier) contacts to semiconducting materials are needed simply to make use of active devices, while both high and low barrier contacts may be employed as active devices themselves (Schottky diodes).

Although the Schottky barrier has been the subject of intensive study for many years, a fundamental understanding of the mechanisms underlying Schottky barrier formation is still lacking. Phenomena intrinsic to an abrupt metal/semiconductor interface can in principle determine the Schottky barrier height.¹ Such phenomena include surface² and interface³⁻⁷ states, interface resonances associated with metal wave-function tails extending into the semiconductor,^{8,9} interface dipole layers,^{3,5,9} surface plasmons,¹⁰ gap closure,¹¹ etc. Even though theoretical calculations of interface electronic structure have illustrated some of these effects and experimental studies have been interpreted as evidence for some of these phenomena, recent theoretical^{7,12} and experimental^{3-5,13,14} work has increasingly emphasized the need for a microscopic understanding of the detailed chemical bonding, and structure, at each specific interface. Nevertheless, characterizing these chemical interactions has proven difficult.

The importance of interfacial chemistry is particularly clear in the case of reactive interfaces. A broad class of metal/Si interfaces (mostly transition metals) is known to be reactive, forming metal-Si compounds (silicides) which grow from the interface.¹⁵ These interfaces have seen increasing application in electronic devices. They represent an attractive subject for Schottky barrier studies as well because: (i) extensive thin film investigations have revealed much about the film growth kinetics, microstructure, and compound phases of the silicide reaction products, and (ii) metal/semiconductor interface chemistry should be simpler

for the elemental semiconductors. Furthermore, the Schottky barrier height of the resulting silicide/Si contact exhibits the importance of the interfacial chemistry in its correlation with silicide heat of formation¹⁶ and eutectic temperature¹⁷.

We have chosen to study the Pd/Si interface because reaction at up to $\sim 700^\circ\text{C}$ yields only a single product¹⁵, Pd_2Si . This choice makes it possible to interpret observations of chemical interactions quite clearly and thus to reveal the initial stages of interface formation. The microscopic chemistry and properties of the Pd/Si interface are dominated by compound formation at the interface, which represents the initial step in the silicide formation reaction.^{18,19} This compound formation seems to be accompanied by stoichiometry variations (Si-excess) in the silicide near the interface and by additional band gap states specifically associated with the interface^{20,21}. These results provide little evidence that phenomena intrinsic to the abrupt interface play an important role in Schottky barrier formation at the Pd/Si interface.

These studies concentrated on the atomically clean Pd/Si(111) and Pd/Si(100) interfaces for very thin ($\leq 1/4\text{\AA}$) as well as thicker metal overlayers. Surface electronic structure was measured by angle-resolved and angle-integrated photoemission spectroscopy (ARUPS and AIUPS respectively) and Auger electron spectroscopy (AES), complemented by transmission electron microscopy (TEM), low energy electron diffraction (LEED), and work-function measurements. Abbreviated descriptions of these results have been published earlier.^{18,19} A discussion of relevant electronic properties of bulk Pd_2Si , based on experimental results described here and on theoretical calculations, is being published separately.²²

II. Experimental Techniques

All depositions and measurements except the TEM studies were carried out in ultrahigh vacuum (UHV, $p \sim 1 \times 10^{-10}$ torr.). Samples were cut from 0.010" thick Si(111) and (100) wafers. The surfaces were cleaned by in-situ ion bombardment. Surface structure damage

was then removed by annealing to $\sim 800-850^{\circ}\text{C}$ for 5-30 min. using direct resistive heating of the sample through Ta clamps holding the sample; visual inspection of the glowing surface during annealing revealed that the sample temperature was quite uniform ($\leq 50^{\circ}\text{C}$) over the entire portion of the surface between the clamps, where spectroscopy measurements were done. The sample temperature was monitored by a chromel/alumel thermocouple spot-welded to one of the Ta clamps; temperatures during annealing were also checked by optical pyrometry.

After the sputter cleaning and annealing, ordered surface structures were observed by LEED. For Si(111), studies on both the (7×7) reconstructed surface and a (1×1) surface (probably representing a disordered (7×7)) were carried out and gave essentially the same results. The Si(100) surface exhibited a $c(4 \times 2)$ superstructure, with $c(4 \times 2)$ LEED spots faint but clearly visible in addition to the (2×1) structure. AES showed the surface to be contaminant-free to about 1% of a monolayer.

Pd overlayers were evaporated by direct sublimation from a resistively heated 0.010" dia. Pd wire. Pd coverages were determined using a quartz crystal microbalance and also by Auger composition analysis; coverages are given in terms of equivalent Pd metal thickness. The Pd source could be maintained at a constant sublimation temperature for a low deposition rate ($\sim 1 \text{ \AA}/\text{min.}$); controlled deposition amounts could then be made by removing a shutter from the evaporant path to the sample for a fixed length of time. In this way relative coverages were accurate to $\sim 10-20\%$ for sequential deposition studies.

UPS measurements were made using a differentially pumped He resonance lamp (HeI, HeII, and NeI lines at incident photon energies $h\nu = 21.2, 40.8,$ and 16.8 eV respectively). For the angle-resolved UPS studies a VG ADES 400 spectrometer was used, while a PHI 15-255G cylindrical mirror analyzer was employed for angle-integrated UPS and AES measurements. Electron counting techniques were used for UPS. The work function ϕ of the surface was obtained from the width of the UPS distribution (secondary electron cutoff to

Fermi energy cutoff), which is simply $(h\nu - \phi)$. Both AES derivative and integrated spectra (dN/dE and $N(E)$ respectively) were measured in analog detection mode with a 5kV primary beam of $\sim 1\mu A$ defocused to $\sim 1mm$ dia.; beam-chopping was employed for the $N(E)$ measurements. AIUPS and AES spectra were acquired into a computer using a device coupler²³; this facilitated the calculation of difference spectra as well as graphics analysis.

TEM studies were carried out after the Pd/Si samples were removed from the UHV system to investigate the compound phases formed, their lattice constants, degree of epitaxy, and interfacial microstructure. Related TEM and AES results on the Pd/Si(111) interface have been published previously.^{18,24}

The surface spectroscopy studies of the interfacial reaction were carried out in two ways. First, progress of the reaction was monitored for relatively thick Pd overlayer films ($\sim 100-300\text{\AA}$) as a function of sequential annealing cycles. Second, the character of the film surface was studied as a function of distance from the interface by observing the spectra after successive depositions of very thin Pd layers ($\sim 1/4\text{\AA}$). These very thin film deposition results reveal in a rather direct fashion the microscopic chemical properties during the initial stages of interface formation. The spectroscopy measurements are sensitive to the interface for metal coverages of order the electron escape depth ($\sim 5 - 25\text{\AA}$); if further metal deposition does not alter the properties of the underlying interface, then these measurements give information characteristic of the buried contact. Furthermore, we note that the interface properties measured here under clean UHV conditions may also be relevant to "real" ("dirty") interfaces: for many cases of silicide formation (including that of Pd_2Si) on contaminated, oxide-covered surfaces, the reaction front moves into the Si substrate to yield a relatively clean silicide/Si interface.¹⁵

III. Results

A. Sequential Annealing of Thick Films

UPS results for successive annealing cycles to react a thick Pd overlayer film illustrate the progress of the reaction and reveal the basic electronic structure of the reaction product, Pd_2Si , as shown in Fig. 1. First a clean, ordered $\text{Si}(111)$ surface was produced and measured, in this case by angle-resolved UPS; the ARUPS properties of this surface were in agreement with those reported previously.²⁵ A relatively thick Pd film ($\sim 300\text{\AA}$) was then evaporated onto the Si substrate which was held at 25°C . The ARUPS spectrum of this overlayer for 15° angle of incidence of the HeI light and normal emission is shown in Fig. 1a. The Pd(4d) bands of Pd metal produce the strong doublet structure seen between -3 eV and -0.5 eV , while a distinct metallic cutoff is observed at the Fermi energy E_F . The work function of this surface, obtained from the width of the UPS spectrum, is $\phi = 5.5\text{ eV}$ as typically observed for evaporated Pd metal. Normal emission spectra like that in Fig. 1a were nearly identical to those for a $\text{Pd}(111)$ single crystal surface²⁶ since the surface of the deposited film is unreacted metal and has strong (111) texture as shown by the TEM studies.

Three successive 150°C annealing steps ($\sim 30\text{ sec}$ each) cause strong modifications in the ARUPS spectrum (Figs. 1b, 1c, and 1d) and reduce ϕ to $\sim 5.04\text{ eV}$; at this point a single peak near -2.75 eV dominates the spectrum and a weak Fermi edge remains. Two further annealing steps shift this peak slightly toward lower energy without further changing ϕ or the overall spectral shape.

TEM analysis carried out after removing the sample from the UHV system determined that the overlayer film whose spectrum is shown in Fig. 1f was continuous and fully reacted to Pd_2Si , with no other phases detectable. As explained below, the surface properties (UPS spectrum and ϕ) for this film were also characteristic of the Pd_2Si bulk of the film. Thus

Pd_2Si has $\phi \approx 5.04$ eV; its UPS spectrum is dominated by a single peak (associated with the $\text{Pd}(4d)$ electrons^{18,22}) near -2.75 eV.

The ARUPS spectra of this Pd_2Si film are insensitive to variations in $h\nu$ (16.8, 21.2, or 40.8 eV), angle of incidence, or angle of emission, in contrast to those for the deposited Pd metal film and for the clean Si surface. This lack of dispersion can be attributed to two factors. First, although thin film studies have established that Pd_2Si can be formed epitaxially on the Si(111) surface,^{27,28} we found that a high degree of epitaxy is not readily achieved for Pd_2Si formation on the atomically clean and ordered Si(111) surface: although $\geq 95\%$ of the silicide could be made epitaxial, values near 30-50% were more typical. Without epitaxy, angular dispersion in ARUPS is expected to be lost. A second explanation for the insensitivity of the ARUPS spectra to angle and to $h\nu$ is that Pd_2Si has a rather large (9 atom) real space unit cell²⁷, and the correspondingly small unit cell in reciprocal space may therefore have many nearly flat bands and exhibit little band dispersion.

Finally, we note that the change in the UPS spectrum of the film surface is rather abrupt: although the annealing steps were all the same in Fig. 1, nearly all changes occur between curves 1b and 1d while only a reduced emission intensity is seen from 1a to 1b and small changes from 1d to 1f. This behavior indicates that the reaction front at which Pd is converted to Pd_2Si is rather sharp. As explained below, it begins at the Pd/Si interface (where Pd_2Si is formed): then the $\text{Pd}_2\text{Si}/\text{Pd}$ interface proceeds through the Pd film toward its surface; when it comes within the UPS detection depth, the spectrum changes markedly.

B. Sequential Deposition of Thin Films—UPS Results

AIUPS spectra for sequential depositions of very thin Pd layers on the clean Si(111) surface at 25°C are shown in Fig. 2. The spectrum for the clean surface shows bulk Si peaks near -7 and -3.5 eV and intrinsic surface state features²⁵ near -1.8 eV and -0.9 eV. The Si(111)-(7 \times 7) surface is known to be metallic²⁵ (the associated metallic Fermi edge is not

clearly observed here because of the modest energy resolution used (~ 0.35 eV) and the disorder of the superstructure which we believe is responsible for the (1×1) LEED pattern seen).

Upon Pd deposition the emission intensity increases significantly due to the considerably larger UPS cross-section of Pd (from its 4d electrons) compared to that of Si. With increasing Pd coverage the intrinsic surface state features are lost and metallic states appear much more clearly at E_F . The bulk Si features observed for $\leq 1\text{\AA}$ metal coverage exhibit no shift in energy, so that no evidence for band-bending changes is found. The work function increases by ~ 0.9 eV. A new peak arises near -3 eV (e.g. see the 1.0\AA curve) and shifts up in energy (toward E_F) slowly. The spectra for $\sim 2\text{--}12\text{\AA}$ closely resemble the ARUPS spectrum of Pd_2Si in Fig. 1f, although relative intensities of various parts of the spectrum differ somewhat. The main peak of Pd_2Si in both AIUPS and ARUPS is asymmetric—sharper on the high energy side and having shoulders near -4.5 eV and -6.3 eV on the low energy side. Auger composition calibrations for films $\sim 5\text{--}10\text{\AA}$ thick like those in Fig. 2 indicated the presence of a Pd-Si layer having about a Pd_2Si stoichiometry on top of the Si substrate. These AIUPS spectra are thus essentially characteristic of Pd_2Si compound.

Although the shift of the main d-band peak from $\sim 2\text{\AA}$ to 12\AA Pd coverage is relatively small, comparable coverage increments from 12 to 22\AA and from 22 to 32\AA produce a more pronounced shift toward E_F . As discussed in detail later, we associate this with the presence of unreacted Pd metal near the surface in addition to Pd_2Si in the film (or possibly Pd-rich Pd_2Si). The AIUPS spectrum is then a combination of the Pd_2Si spectrum (d-band peak near -2.75 eV) and a Pd spectrum (center of mass of d-band structures near -1.75 eV) so that the main peak occurs somewhere in the middle (~ -2.0 eV for 32\AA coverage). Since silicide formation begins at the Pd/Si interface and proceeds through the Pd film, progressively less reaction may have taken place at positions further from the interface (which are seen in the surface spectra for higher coverage).

In order to better understand and interpret the changes in the UPS spectra—especially for low coverage—we concentrate on "difference spectra". Because the Pd cross-section is much larger than that for Si, the difference curve obtained by subtracting the clean Si spectrum from the Pd-covered spectrum is nearly the same as the Pd-covered spectrum itself if the coverage is $\geq 4\text{\AA}$. Corresponding difference curves for lower coverage show the electronic structure changes associated with all the deposited Pd present at that point. However, even more revealing information can be obtained from "incremental difference curves" such as those shown in Fig. 3b, 3c, and 3d for Pd/Si(111); these are representative of electronic structure changes associated with additional 0.25\AA Pd coverage increments deposited on top of whatever Pd was already present. These difference curves are compared to the spectra for clean Si(111) and those for 4\AA and 12\AA Pd/Si(111) in Fig. 3.

Although not at all obvious from the spectra in Fig. 2, the difference spectra in Fig. 3 show clearly that the electronic structure associated with submonolayer amounts of Pd deposited on Si(111) closely resembles that of Pd_2Si (Fig. 3f), with a weak Fermi edge and a strong asymmetric peak (high energy side sharper) $\sim 3\text{ eV}$ below E_F . This marked similarity leads us to conclude that chemical bonding at very low coverage is very similar to that in Pd_2Si (as seen by UPS), i.e. a Pd_2Si -like compound is formed. We note, however, that there are some differences between the electronic structure at very low coverage and that of bulk Pd_2Si . The d-band peak shifts from an initial position at -3.5 eV (Fig. 3b) continuously toward E_F with higher coverage, reaching $\sim -2.75\text{ eV}$ in bulk Pd_2Si for $\geq 10\text{\AA}$ coverage. Furthermore, the intensity near E_F , i.e. in the Si band gap region, appears somewhat enhanced at low coverage relative to the main d-band peak.

Corresponding AIUPS results for very thin Pd layers on the clean Si(100) surface are shown in Fig. 4. Intrinsic surface state features exist²⁹ near -0.7 eV and -1.3 eV ; the latter is seen clearly in Fig. 4a and gives rise to a marked dip at this energy in the difference spectra (Figs. 4b and 4c). In spite of the differences between the initial clean Si(111) and (100)

surfaces, the results are very similar. On the (100) surface, as on the (111) surface, the Pd_2Si spectrum is observed at $\sim 12\text{\AA}$ Pd coverage. The low coverage difference spectra on $\text{Si}(100)$ also show the essential Pd_2Si spectral characteristics, including a well-defined Fermi edge, a strong d-band peak near -3 eV , and the shift of this peak from $\sim -3.5\text{ eV}$ at lowest coverage to a final position near -2.75 eV at higher coverage. Silicide formation thus occurs in a very similar way on $\text{Si}(100)$ as on $\text{Si}(111)$.

The low-coverage UPS spectra are much more similar to those for bulk Pd_2Si than to those for very thin overlayers of pure transition metals. The UPS spectra for thin Pd layers on Ag^{30} and Pd alloyed with Ag^{31} show resonant d-levels with widths and binding energies below E_F ($\sim 1\text{ eV}$) which are $\sim 2\text{-}3\text{X}$ smaller than observed here for Pd on Si. Thin $\text{Pd}(111)$ overlayers on $\text{Nb}(110)$ exhibit d-levels at $\sim -3.1\text{ eV}$, again with a smaller width ($\sim 0.5\text{ eV}$) than that for Pd/Si .³² In both cases the coverage-dependent shifts of the d-level are much smaller ($< 0.2\text{ eV}$) than those seen here ($\sim 0.75\text{ eV}$). Very thin (≤ 1 monolayer) Pd films on polar ZnO surfaces³³ do not react strongly with the ZnO ; again the Pd d-bands differ markedly from the low-coverage Pd/Si spectra, with $\sim 2\text{-}3\text{X}$ narrower peak width and with peak asymmetry of the opposite sign. Thus experimental UPS results provide no evidence favoring the presence of an elemental Pd film at low coverage. Such a hypothesis is also contradicted by the existence of epitaxy for Pd_2Si on $\text{Si}(111)$ and by the formation of Pd_2Si observed directly at higher coverage.

On crystalline graphite surfaces the Pd d-levels at low coverage (in He I UPS spectra) appear near -2.5 eV and shift somewhat ($\sim 0.5\text{ eV}$) toward E_F with increasing coverage.³⁴ Their width is also comparable to that for Pd/Si . Thus the Pd d-band behavior at low coverage is similar on Si and graphite surfaces, but this could also result from similar chemical bonding and stoichiometry effects in a mixed Pd-Si or Pd-C interfacial material, especially because Si and C are isoelectronic.

We conclude that a Pd_2Si -like compound is formed at low coverage insofar as its electronic structure as seen in UPS is concerned.

C. Sequential Deposition of Thin Films—AES Results

The Si $L_{2,3}\text{VV}$ Auger spectrum provides a valuable measure of interface electronic structure because: (i) it is clearly sensitive to the chemical environment of the Si atom and its local valence bonding; (ii) its lineshape is bandlike (i.e. revealing density-of-states information) rather than quasi-atomic; and (iii) it is atom-specific, showing local density-of-states properties at the Si site—in complementary relation to the UPS valence band spectra, which reveal mainly Pd d-band features. Other Auger transitions involving the valence band are either quasi-atomic (e.g. the Pd $M_{4,5}\text{VV}$ near 330 eV) or otherwise not satisfactory for studies of the initial stages of interface formation because they are too weak (e.g. the Si KLV near 1650 eV) or overlapping with other Auger transitions (e.g. the Si $L_1L_{2,3}\text{V}$ near 50 eV).

The Si $L_{2,3}\text{VV}$ AES spectra for the clean Si(111) surface and for thin Pd layers deposited at 25°C are shown in Fig. 5 (undifferentiated or $N(E)$ mode). The spectra all have a common zero for $N(E)$. The dominant peak in the clean spectrum, at ~88.5 eV, is replaced by four new features at ~94, 89.5, 85, and 80 eV, as Pd is deposited on the surface. Since this Si AES transition is observed for thicknesses $\geq 30\text{\AA}$, which are large compared to its Auger escape depth (~7\AA in elemental Si), Si is present in the deposited overlayer. Auger composition analysis has demonstrated²⁴ that the stoichiometry of overlayers formed in this way for $\geq 3\text{-}5\text{\AA}$ Pd coverage is essentially that of Pd_2Si , and TEM analysis of such samples confirms the existence of the Pd_2Si lattice structure. The spectrum in Fig. 5f thus represents that of bulk Pd_2Si . The interpretation of its features has been discussed previously²²; they involve mainly the Si(3p)-Pd(4d) bonding and antibonding valence state which determine the cohesive energy and phase stability of the Pd_2Si compound.

Because of the proximity of the Si 88.5 eV and the Pd₂Si 89.5 eV peaks (which are respectively suppressed and enhanced with Pd coverage), standard difference curves (Pd-covered minus clean surface spectra) and incremental difference curves (as used in the AIUPS results in section IIIB) would be misleading. We therefore analyze the AES spectra for the initial stages of interface formation by decomposing the N(E) spectra into a portion due to elemental Si and a portion due to the Pd₂Si-like compound. Since the elemental Si part corresponds to Si below the overlayer, its shape will remain constant (that seen in Fig. 5a) while its intensity decreases with overlayer thickness. Since there is no evidence for band-bending changes from UPS, we assume that the elemental Si contribution remains unshifted for decomposing the AES spectra.

The decomposition of the Si L_{2,3}VV spectra in Fig. 5 into Pd₂Si and elemental Si contributions is shown in Fig. 6. It is clear that, as in the AIUPS results, the essential features of the bulk Pd₂Si spectrum dominate the interface electronic structure observed at very low Pd coverage (these AES results would be inconsistent with a hypothesis that a very thin elemental Pd film is formed at low coverage). However, some differences (as in the AIUPS results) are found between the low coverage spectra and the bulk Pd₂Si spectra. The 94 eV peak (and possibly the 79 eV peak) shift toward higher energy with increasing coverage. The intensity of states nearest E_F (reflected in the highest-energy AES structure at ~94 eV) decreases with increasing coverage relative to the other peaks at lower energy. Like the AIUPS results, these spectra indicate that a Pd₂Si-like compound is formed in the initial states of interface formation.

D. Work Function Measurements and Schottky Barrier Height

By monitoring the shift of the secondary electron cutoff (i.e. changes in the width of the UPS spectrum), work function changes as small as ~30-50 meV could be detected. Since the Pd sublimation rate could be maintained constant over many thin layer evaporations, the

change in work function with coverage could be measured in considerable detail, as shown in Fig. 7. With increasing Pd coverage ϕ increases monotonically from its value for the clean Si(111) surface (4.6 eV²⁵) to that of Pd₂Si (~5.04 eV) in ~10-12Å, then rises more slowly with further Pd coverage. The shaded ϕ region, ~5.0-5.1 eV, represents approximately the range of bulk Pd₂Si work functions, as described in section IIIE. For Pd coverages above ~10-15Å deposited at room temperature, ϕ increases toward that of Pd metal (~5.6 eV) due to the presence of incompletely reacted Pd metal at the surface of the overlayer. This is consistent with the coverage-dependence of the main d-band peak position seen in AIUPS (section IIIB).

The ϕ behavior in Fig. 7 shows a delayed onset of ϕ changes, and ϕ does not reach its Pd₂Si value until ~8-10Å Pd coverage. Two factors may influence this behavior. First, the UPS measurement of the surface work function concentrates on the threshold or cutoff of the secondary electron distribution. If the surface consists of patches of material having different ϕ values (e.g., some clean Si and some Pd₂Si), the measurement will be much more sensitive to the lower ϕ material, which determines the actual cutoff. This fact may explain why the onset of work function changes is delayed until ~2Å Pd coverage. However, this effect appears incapable of explaining why the Pd₂Si work function is not obtained by ~3-5Å coverage, since TEM observations for this coverage showed the overlayer to be continuous.

The second factor which could account for both the delayed onset of work function changes and the delay in attaining $\phi = \phi_{\text{Pd}_2\text{Si}}$ is that the material produced at the interface—i.e., in the initial stages of interface formation—may differ somewhat from bulk Pd₂Si. This would be consistent with the differences (discussed in sections IIIB and IIIC) in the AIUPS and AES spectra for very low Pd coverages compared to those for bulk Pd₂Si. Since ϕ for a Pd-Si mixture or compound most likely scales monotonically with concentration between the work functions of the elemental constituents, a plausible interpretation of the delay in reaching $\phi_{\text{Pd}_2\text{Si}}$ is that the material produced near the interface has a larger Si/Pd

concentration ratio that that in Pd_2Si —i.e., it is Si-rich Pd_2Si . This possibility is discussed more thoroughly in section IVB.

It is interesting to compare the Schottky barrier height of these atomically clean interfaces with thick film results obtained under more usual processing conditions. The barrier height of the contact is given by the value of the clean Si surface modified by the metal-induced change in band-bending. For the clean n-Si(111) surface, we take the Schottky barrier height to be $E_c - E_F = 0.79 \text{ eV}^{35,36}$ (where E_c is the energy of the conduction band minimum at the surface); for n-Si(100) it is similar²⁹ ($0.75 \pm 0.15 \text{ eV}$). The metal-induced change in band-bending can in principle be obtained from the shift in a bulk Si UPS feature; using the bulk structures near -7 eV for the clean Si(111) and Si(100) surfaces, the band-bending is unchanged by Pd deposition (to $\pm 0.1 \text{ eV}$). (Above $\sim 1\text{\AA}$ Pd this peak is not easily distinguished so that further band-bending changes are not measured). This would give a Schottky barrier height for the Pd_2Si film on both the clean Si(111) and Si(100) surfaces of $\sim 0.79 \pm 0.1 \text{ eV}$, in good agreement with thick film results.¹⁶ This agreement may result from the fact that the Pd/Si interfacial reaction occurs whether or not native oxides and/or contamination are present, producing regions of relatively clean Pd_2Si /Si interface which determine the electrical properties.

E. Interface and Film Reaction Kinetics—Effects on Surface Spectroscopies

It is worthwhile to emphasize the rapid reaction kinetics observed here for Pd_2Si formation. Although thin film investigations have shown that 200°C annealing is required to form Pd_2Si from $\geq 1000\text{\AA}$ Pd film deposited under modest vacuum conditions onto substrates prepared by standard processing techniques (wet chemical etch, etc.), we find spontaneous Pd_2Si formation within $\sim 10\text{--}20\text{\AA}$ of the initial interface at 25°C . In fact, we also carried out AIUPS experiments with the Si(111) sample held at $\sim 180^\circ\text{K}$ and obtained results essentially identical to those in Fig. 2, suggesting that silicide is formed even at low temperature in basically the same way as at room temperature.

The fast reaction kinetics observed here cannot be directly compared with standard thin film studies for three reasons. First, the present studies concentrate on much thinner films, so that mass transport (believed to be the rate-limiting step in relatively thick Pd_2Si film growth) may be less important. Second, these experiments have been carried out on atomically clean and ordered Si surfaces under UHV conditions which allow Pd deposition without significant interface contamination, so that the kinetics of interface reaction steps in the Pd_2Si formation process may thus be much faster and could even be qualitatively different. Third, the present experiments concentrate in fact on the initial stages of silicide formation, in which at low coverage Pd_2Si is produced at the Pd/Si interface; in contrast, the Pd_2Si growth process for thicker films involves interface reaction steps at the Pd/ Pd_2Si and the Pd_2Si /Si interfaces in addition to mass transport.

Since the silicide formation reaction originates at the Pd/Si interface, temperature dependence and thermal history will strongly influence what phases are present at various distances from the initial interface. In order to safely use the surface spectroscopy results, we must therefore be sure that the surface region from which spectra are obtained are composed of the phases we identified, e.g. for the full overlayer film by TEM. The results of this analysis are especially important because we attempt to first identify the UPS and AES features characteristic of the bulk silicide product (Pd_2Si) and then to interpret the interface electronic structure (low-coverage spectra) on the basis of their comparison with the bulk silicide electronic structure.

An example of this problem was already shown and discussed in conjunction with Fig. 2. As the Pd coverage is increased above $\sim 12\text{\AA}$ the main d-band peak of Pd_2Si appears to shift closer to E_F ; this is because at 25°C the reaction has not gone to completion at the outer surface of the overlayer. Here unreacted Pd metal is mixed with Pd_2Si (or possibly the Pd_2Si is Pd-rich), giving a composite surface spectrum with a d-band peak position between that of Pd_2Si and Pd metal.

Other examples of this "under-reaction" condition of the surface are illustrated by two dashed curves in Fig. 8, which correspond to different Pd coverages deposited at room temperature. It is clear that the d-band peak position can be varied continuously from ~ -3.5 to ~ -1.5 eV by changing the coverage for a 25°C deposition temperature. In contrast, we found that a brief (\sim few minutes) annealing at $\sim 200^\circ\text{C}$ returns surface spectra essentially to that of Pd_2Si , as indicated by the solid curve in Fig. 8 as well as the 12\AA curve in Fig. 2.

Figure 7 shows that the work function behavior with coverage changes at $\phi \approx 5.0-5.1$ eV, indicating a ϕ value in this range for bulk Pd_2Si . Since both the work function and the d-band peak position E_{PEAK} are sensitive to and vary with Pd coverage (but in different ways), we used their correlation to determine ϕ and E_{PEAK} characteristic of bulk Pd_2Si . This relation is depicted in Fig. 9a for Pd/Si(111). The very thin film deposition results are shown by solid dots, and E_{PEAK} in this case corresponds to the d-band peak position from the incremental difference curves. As also seen in Fig. 7, ϕ increases from the clean Si(111) value (4.6 eV) to ~ 5.04 eV as the E_{PEAK} increases. Once $\phi \approx 5.04$ eV is reached, ϕ increases only very slowly while E_{PEAK} shifts closer to E_F with the presence of additional unreacted Pd metal at the surface; this unreacted metal makes a direct contribution to shifting the peak but does not change ϕ significantly because $\phi_{\text{Pd}} \approx 5.6$ eV, considerably larger than $\phi_{\text{Pd}_2\text{Si}} \approx 5.04$ eV. This behavior is a clear indication that the surface is composed of Pd_2Si regions and unreacted Pd metal regions.

The thick film annealing behavior is also depicted in Fig. 9a, by open circles and triangles. In this case ϕ starts from about the Pd metal value and decreases to the Pd_2Si value as the silicide formation reaction reaches the top surface. Note that in both the thick film annealing and thin film deposition results ϕ reaches a plateau at the same value, $\phi \approx 5.04$ eV. We therefore identify this as $\phi_{\text{Pd}_2\text{Si}}$. This state of the surface occurs for $E_{\text{PEAK}} \approx -2.75$ eV, which thus represents the d-band peak position for bulk Pd_2Si . The area enclosed by the

dashed line in Fig. 9a indicates an approximate parameter space in which the surface region of a Pd_2Si film is essentially Pd_2Si , like the underlying bulk.

The ϕ vs. E_{PEAK} results for $\text{Pd}/\text{Si}(100)$ are shown in Fig. 9b. The behavior is similar to that of $\text{Pd}/\text{Si}(111)$ except that the initial work function for the clean surface is higher.

These results demonstrate that the "under-reaction" or Pd surface enrichment problem at the top surface occurs at 25°C only if the film is $\geq 10\text{-}15\text{\AA}$; at lower coverage the top surface is sufficiently close to the initial Pd/Si interface that all the Pd is converted into Pd_2Si form by the interface-driven reaction. With annealing for several minutes at $150\text{-}200^\circ\text{C}$, a thicker overlayer can be transformed completely into Pd_2Si .

Annealing at still higher temperatures like 400°C (or possibly much longer annealing times at $\sim 200^\circ\text{C}$) produces yet a different effect, as shown by the dotted AIUPS curve in Fig. 8. The lineshape changes somewhat and the emission intensity is reduced considerably. The correlation between the AIUPS and the AES spectral changes, depicted in Fig. 10, demonstrates that the 400°C annealing cycle ("over-reaction" condition) decreases the Pd/Si concentration ratio at the surface dramatically.³⁷ It also returns the Si $L_{2,3}\text{VV}$ AES lineshape to its elemental Si form, suggesting that the surface layer(s) may be relatively free of Pd and perhaps covalently bonded. Finally, we note that exposure of this "over-reacted" surface to oxygen produces an AIUPS spectrum like that resulting from oxygen exposure to the clean Si surface; in contrast, the Pd_2Si surface formed by 200°C annealing is relatively inert to oxygen exposure.

Whereas the cause of the "under-reaction" condition (Pd surface enrichment) is clearly the fact that the silicide formation rate is lower further from the interface, the cause of the "over-reaction" condition (Si surface segregation) is less obvious. One possibility is that the solubility of Si in Pd_2Si is temperature-dependent, so that at 400°C more Si dissolves and must then segregate back into the Si or to the Pd_2Si surface upon cooling to 25°C (at which

the measurements were made). This possibility is being checked experimentally. Alternatively, the surface free energy may be reduced (for some unknown reason) by the presence of a Si layer at the vacuum interface.

IV. Discussion

A. Reaction Behavior

The UPS and AES spectra presented here demonstrate clearly that the clean Pd/Si interface is reactive. As emphasized by previous work,³⁻⁵ this implies that a meaningful understanding of the Pd/Si Schottky barrier requires detailed knowledge of the microscopic interfacial chemistry. By measuring the dependence on reaction parameters such as temperature, source supply (here Pd thickness), etc., it has been possible to determine how the state of the system varies with these parameters, then to deduce the surface spectroscopic properties of the Pd₂Si reaction product, and from this to have a basis for interpreting observations of the initial stages of interface formation.

Although some characteristics of the very low coverage results remain to be discussed in detail and evaluated below, it is clear from section III E that a well-defined Pd₂Si compound is formed at $\sim 3\text{-}12\text{\AA}$ Pd coverage from $\sim 180^\circ\text{K}$ to \sim room temperature. At higher coverage the surface of the overlayer becomes partially unreacted. The reaction product and processing temperatures are similar on the atomically clean Si(111) and Si(100) surfaces. The evolution of the partially unreacted surface for sufficiently thick films at $\sim 25^\circ\text{C}$ demonstrates that the initial stage of the silicide formation reaction (Pd₂Si formation at the Pd/Si interface) proceeds considerably faster than the growth rate of thicker silicide films (i.e. after some Pd₂Si is present). This may be a consequence of the heat of adsorption of Pd on Si, the energy of which could be sufficient to promote the initial reaction step spontaneously even at low temperatures.

B. Low Coverage Reaction Product

As discussed earlier, the evidence supports an identification of the interfacial material formed at low coverage as a Pd_2Si -like compound. First, the low coverage UPS and AES spectra (difference curves) are strikingly similar in shape to those for bulk Pd_2Si . Second, this similarity holds both for the Si local density-of-states (as seen in the Si $L_{2,3}\text{VV}$ AES spectrum) and for the Pd density-of-states (which dominates the UPS spectrum). Recent TEM vertical sectioning results^{38,39} for the buried interface show the lattice fringes of the Pd_2Si overlayer and the Si substrate continuing to an atomically abrupt interface. Identifying the low-coverage reaction product as a Pd_2Si -like compound provides a reasonable starting point for the abrupt buried interface, for the interface-driven character of the reaction, and for epitaxial Pd_2Si growth on Si(111). It also gives physical insight into the microscopic chemical origin of the interface electronic structure observed during the initial stages of interface formation; it says essentially that the metal-induced states at the interface are primarily those of the Pd_2Si -like compound formed.

C. Spectroscopically Observed Chemical Shifts

However, the low-coverage spectra are not completely equivalent to those of bulk Pd_2Si . The d-band peak position in UPS appears ~ 0.75 eV further below E_F than in Pd_2Si and shifts smoothly with coverage. With increasing coverage, the highest-energy AES peak near 94 eV also shifts toward higher energy and decreases in intensity relative to the other AES peaks. As explained previously,²² this peak is associated with Si(3p)-Pd(4d) antibonding states, so that its energy shifts may be related to those of the main d-band peak observed in the UPS spectrum.

It is interesting to note that these chemical shifts seem to persist to Pd coverages considerably larger than both the first monolayer or so and also the screening length ($\sim 1\text{\AA}$) in the metallic Pd_2Si film. In the AES spectra (Fig. 6), the position and relative intensity of the 94 eV peak continue to change even out to 30\AA Pd coverage. Since this particular feature of the Si $L_{2,3}\text{VV}$ AES spectrum is associated specifically with those Si atoms bonded to Pd in silicide

form, these variations are relatively free of complications from the "under-reaction" and "over-reaction" phenomena discussed in section III E. In the UPS spectra (Figs. 3 and 4), the d-peak shifts are most dramatic in the first Å but are still clearly evident at $\sim 12\text{Å}$ coverage. The UPS shifts persist on fully reacted Pd_2Si films to $\sim 100\text{Å}$,¹⁸ although a slight "under-reaction" or "over-reaction" condition could contribute to an apparent peak shift in these measurements. We recognize, however, that the smaller peak shifts observed in the 10 - 100 Å coverage range are further complicated by the finite electron escape depth ($\sim 7 - 20\text{ Å}$), which can broaden the coverage range over which peak shifts are detected.

1. Interface Strain

Strain caused by lattice mismatch at the interface could alter the electronic structure near the boundary and cause changes for tens of Å or more from the interface. For $\text{Pd}/\text{Si}(111)$ (the epitaxial case) the Pd_2Si basal plane lattice constants were in fact found to increase at low coverage toward the $\text{Si}(111)$ value, and at the same time the d-band peak shifted to larger binding energy. However, virtually identical d-peak shifts with coverage are observed (Fig. 4) for $\text{Pd}/\text{Si}(100)$, where no epitaxial relationship exists and interface strains should be different. Unless the $\text{Pd}/\text{Si}(100)$ interface would be drastically reconstructed to consist of $\text{Pd}/\text{Si}(111)$ facets, it is difficult to accept interface strain as the explanation for the coverage-dependent chemical shifts.

2. Stoichiometry Variations

An attractive explanation for these chemical shifts is stoichiometry changes within the Pd_2Si compound near the interface. The Si concentration gradient across an abrupt $\text{Pd}_2\text{Si}/\text{Si}$ interface seems a logical driving force for motion of Si atoms across the boundary. In this way Si-rich Pd_2Si would be produced near the interface with a stoichiometry in the Pd_2Si graded over $\sim 10\text{-}100\text{Å}$ to reduce the local Si concentration gradient throughout the film. The

low-coverage spectra would reflect the Si-rich stoichiometry of the Pd_2Si compound formed, and with increasing coverage the surface region measured would be further from the Pd/Si interface and thus less Si-rich, presumably reaching exactly Pd_2Si for very thick, fully-reacted overlayers.

Evidence supporting this explanation comes from three sources. First, self-consistent calculations for several Pd-Si compounds of different stoichiometry have revealed how density-of-states features in Pd-Si compounds change with stoichiometry.²² These calculations employed the Augmented-Spherical-Wave method and treated Pd_3Si , PdSi , and PdSi_3 compounds in the Cu_3Au , CuAu , and CsCl structures, with lattice constants determined by total energy minimization. For Pd_3Si , the local Si environment (only Pd nearest neighbors) was close to that in Pd_2Si . Although details of the calculated density-of-states changed somewhat with crystal structure for a given compound, the essential qualitative features of the Pd-Si chemical bonding were unaffected, and overall energy positions of structure did not change dramatically with reasonable variations in lattice constant. Furthermore, the calculated densities-of-states are consistent with more detailed self-consistent calculations of the real Pd_2Si compound carried out by Pandey.⁴⁰

These results illustrate the qualitative effects of stoichiometry changes clearly. The Pd-Si bonding occurs by the formation of $\text{Pd}(4d)-\text{Si}(3p)$ bonding and antibonding states which lie respectively below and above the main $\text{Pd}(4d)$ peak in the total density-of-states.²² With increasing Pd concentration, the antibonding states and the main $\text{Pd}(4d)$ peak shift toward higher energy; in going from PdSi to Pd_3Si , the antibonding states become empty. Phase stability may be expected when a fraction of the antibonding states are emptied, so that from these calculations a stable stoichiometry might be anticipated somewhere between PdSi and Pd_3Si ; this agrees with the fact that Pd_2Si is the stable compound. The observed UPS shift of the main d-band peak up toward E_F with increasing coverage and its interpretation as a decrease in the Si excess of the Pd_2Si (i.e. increased Pd concentration) is consistent with the

trends predicted by these calculations, as is the shift of the Si $L_{2,3}$ VV 94 eV peak toward higher energy with coverage.

The second body of evidence that the chemical shifts arise from stoichiometry variations in the Pd_2Si film comes from measurements of the spectra⁴¹⁻⁴⁴ of $Pd_{1-x}Si_x$ metallic glasses, which occur over the range $x \sim 0.15-0.25$. For these Pd-Si mixtures, which are richer in Pd than is Pd_2Si , the main d-peak occurs within ~ 2 eV of E_F , i.e. closer to E_F than observed here for Pd_2Si . Furthermore, the UPS lineshape and work function are very similar to that for Pd_2Si . Finally, the d-peak moves monotonically upward toward E_F with increasing Pd concentration of the metallic glass.⁴⁴ These observations are all consistent with the calculations²² and with our interpretation that the low coverage Pd/Si spectra represent more Si-rich Pd_2Si than the truly stoichiometric compound and that the amount of Si excess in the well-defined Pd_2Si film decreases with coverage or distance from the interface. Extrapolating from the d-peak shift with concentration in the metallic glasses,⁴⁴ the apparent concentration seen by UPS at lowest coverage might be as high as $\sim 45-60\%$ Si; at higher coverage ($\geq 4\text{\AA}$) where smaller chemical shifts from bulk Pd_2Si positions are observed, the Si concentration should be not more than a few % Si excess for unannealed samples.

The third source of evidence supporting stoichiometry variations in the Pd_2Si overlayer film comes from TEM measurements of the basal plane lattice constants $a_0/2$ of fully reacted Pd_2Si films on Si(111).¹⁸ These show that with increasing Pd_2Si film thickness from 20\AA to 300\AA the $a_0/2$ value decreases from 6.58 to 6.52\AA ; at the same time the d-peak position shifts toward E_F from -2.93 eV to -2.76 eV. X-ray powder studies⁴⁵ have indicated that larger $a_0/2$ values are obtained for "Si-rich" than for "Pd-rich" Pd_2Si , although measurements were confined to the range $a_0/2 = 6.50-6.52\text{\AA}$ and stoichiometry was not quantified. This would suggest that at lower coverage, where larger d-peak binding energies and corresponding larger $a_0/2$ values are observed, the Pd_2Si is more Si-rich than at higher coverage.⁴⁶

Thus it seems reasonable to interpret the coverage-dependent chemical shifts as evidence that a Si-rich Pd_2Si -like compound is formed at very low coverage and that the amount of Si excess in the Pd_2Si overlayer decreases with distance from the interface. This inference forms a considerable part of the basis for a theory of silicide Schottky barriers proposed by Freeouf.⁴⁷ In this theory, the work function on the metal side of the contact is shifted from a silicide value considerably toward that of elemental Si by the Si-rich stoichiometry of the silicide at the interface; the Schottky barrier height, which scales with the work function difference across the interface in a simple Schottky picture,⁴⁸ then exhibits considerably less variation with different metal silicides than would be expected from metal or metal silicide work functions.

3. Chemical Environment and Interface State Effects

For the low-coverage regime there exist other explanations for the relatively large chemical shifts observed with coverage, based on the specific chemical environment of atoms nearest the interface. First, Pd-Si bonds in the silicide closest to the Si substrate may appear in these electron spectroscopy measurements to be in a Si-rich environment due to the elemental Si charge density which forms part of that environment. Second, some of the Pd-Si bonds may differ from those of the bulk silicide due to particular structural arrangements present only near the interface. Third, a high density of metal atom interstitials within the Si lattice could appear spectroscopically as a Si-rich silicide.⁴⁹ Differentiating between true stoichiometry variations, local chemical environment effects, and altered interface bonding arrangements in the low-coverage regime represents a difficult semantic and conceptual, as well as experimental, task, so we cannot at present suggest which of these pictures (if any) is more meaningful and accurate an explanation for the chemical shifts observed at low coverage.

Other electronic states in the band gap may be produced near the interface in addition to the metallic states of the bulk silicide. This can be inferred from differences between the low

coverage spectra and the bulk Pd_2Si spectra in the Si band gap region. Besides the shift of the 94 eV peak (associated with states just below E_F) in the Si $L_{2,3}\text{VV}$ AES spectrum toward higher energy with increasing coverage (Fig. 6), its intensity is enhanced at low coverage relative to other peaks in the spectrum (this effect has been noted previously by Roth and Crowell⁵⁰). That the enhancement is more readily seen in the AES spectra than in UPS may result from the fact that the Si $L_{2,3}\text{VV}$ AES spectrum is specific to the local Si atom density-of-states (much of which is concentrated in the bonding and antibonding bands), while the UPS spectra are dominated by much stronger Pd d-electron contributions elsewhere in the spectrum. This enhancement of the density-of-states in the band gap region (near E_F) may represent additional states characteristic of the interface. Such states could provide an alternative explanation for the spectroscopically observed chemical shifts as well as for the enhancement of the 94 eV AES peak. This question deserves further detailed study in the future.

V. Conclusions

The main conclusions of this study may be summarized as follows:

1. Silicide compound formation (Pd_2Si) dominates the microscopic chemistry and properties of the clean Pd/Si interface.
2. Consequently, the interface electronic structure in the initial stages of interface formation—and presumably for the thick metal contact (buried interface) as well—is primarily that of Pd_2Si : strong Pd(4d) bands about 3 eV below E_F with bonding Pd(4d)-Si(3p) bands below and corresponding antibonding bands near E_F forming the conducting states of the metallic Pd_2Si compound.
3. Reactivity at the clean interface is very high: silicide formation occurs spontaneously at the interface even at temperatures as low as 180°K.
4. Coverage-dependent chemical shifts in the spectroscopy measurements can be interpreted as evidence for interface-driven stoichiometry variations in the Pd_2Si

overlayer; these would consist of Si-rich Pd_2Si near the interface, with a graded stoichiometry (Si excess) which decreases with distance from the interface.

5. The observed work function behavior can be fully understood on the basis of Pd_2Si compound formation and the thin film kinetics phenomena (Pd surface enrichment due to incomplete reaction, Si surface segregation by "over-reaction") which occur. As a result, the ϕ behavior provides no direct evidence for interface dipole formation (although such a contribution cannot be ruled out); instead, it gives a very sensitive measure of the thin film reaction kinetics and surface segregation phenomena.
6. As a consequence of interface reactivity, the reaction kinetics of the thin overlayer film becomes an important experimental complication, especially when surface-sensitive spectroscopic techniques like UPS and AES are used. However, by studying the dependence on thermal history, it is possible to obtain reliable results from these techniques.

This study has produced a relatively simple picture of the microscopic chemical behavior at the Pd/Si interface, in which compound formation has been clearly identified and plays a dominant role in determining the interface electronic properties. This suggests the possibility that similar chemical processes might equally well explain previous results in other metal/semiconductor systems. For example, Pd-GaAs reactions are known to produce various compounds⁵² like Pd_2Ga , PdGa , and PdAs_2 . The UPS difference spectrum for 2-3 monolayers of Pd on GaAs(110)⁵³ is very similar to that of Pd_2Si : its dominant d-peak occurs at ~ -2.5 eV with a full width at half maximum of ~ 3 eV. This suggests that compound formation may take place at the Pd/GaAs(110) interface, although the identity of the reaction product is not known.

The insight which has come from the present study of the Pd/Si interface partly results from the fact that the chemical reaction is simple, producing a single product— Pd_2Si . This characteristic was anticipated from previous thin film studies (albeit under less controlled

interface conditions) and played an important role in the choice of this particular reactive interface. Although some of the other silicide-forming interfaces may produce multiple products, rather extensive thin film results are available for such systems.

In contrast, no bulk compounds are known for the simple metals (Al, Ga, and In) on Si. This makes it difficult to characterize what (if any) chemical reactions may have occurred at the corresponding interfaces. Identifying reactions at compound semiconductor interfaces is made difficult by (i) the larger number of possible reaction products, (ii) the simultaneous presence of several reaction products, and (iii) the possibility of preferential surface segregation^{54,55}. This underscores the need for more thin film investigations of reactions between metals and compound semiconductors. In spite of these problems, significant progress has been made in identifying chemical reactions at clean metal/III-V semiconductor interfaces, such as the exchange reaction for Al/GaAs.⁵⁶

The results presented in this paper have demonstrated that surface spectroscopy techniques can reveal the microscopic chemical processes occurring at the reactive metal/Si interface and display many aspects of the interface electronic structure. The further challenge is to develop reliable techniques for in-situ monitoring of changes in the Schottky barrier height at low metal coverage and/or to correlate the interface electronic properties and microstructure with the electrical properties of the bulk contact, so that the mechanism(s) which really determine the Schottky barrier height can be identified.

References

* Supported in part by the Office of Naval Research.

1. See, e.g., J. Vac. Sci. Technol. *11*, 935-1028 (1974).
2. J. Bardeen, Phys. Rev. *71*, 717 (1947).
3. G. Margaritondo, J. E. Rowe, and S. B. Christman, Phys. Rev. B *14*, 5396 (1976).
4. J. E. Rowe, S. B. Christman, and G. Margaritondo, Phys. Rev. Letters *35*, 1471 (1975); G. Margaritondo, S. B. Christman, and J. E. Rowe, J. Vac. Sci. Technol. *13*, 329 (1976).
5. L. J. Brillson, J. Vac. Sci. Technol. *15*, 1378 (1978); Phys. Rev. Letters *40*, 260 (1978); Phys. Rev. B *18*, 2431 (1978).
6. R. Ludeke, Phys. Rev. Letters *39*, 1043 (1977).
7. H. I. Zhang and M. Schlüter, Phys. Rev. B *18*, 1923 (1978); J. Vac. Sci. Technol. *15*, 1384 (1978).
8. V. Heine, Phys. Rev. *138*, A 1689 (1965).
9. J. Ihm, S. G. Louie, and M. L. Cohen, Phys. Rev. B *18*, 4172 (1978).
10. J. C. Phillips, Phys. Rev. B *1*, 593 (1970).
11. J. C. Inkson, J. Phys. C *5*, 2599 (1972); J. Phys. C *6*, 1350 (1973); J. Vac. Sci. Technol. *11*, 943 (1974).
12. J. C. Phillips, J. Vac. Sci. Technol. *11*, 947 (1974).
13. P. W. Chye, I. Lindan, P. Pianetta, C. M. Garner, C. Y. Su, and W. E. Spicer, Phys. Rev. B *18*, 5545 (1978).
14. R. H. Williams, V. Montgomery, and R. R. Varma, J. Phys. C *11*, L735 (1978).
15. K. N. Tu and J. W. Mayer, in *Thin films—Interdiffusion and Reactions*, edited by J. M. Poate, K. N. Tu, and J. W. Mayer (Wiley, New York, 1978), p. 359.
16. J. M. Andrews and J. C. Phillips, Phys. Rev. Letters *35*, 56 (1975).
17. G. Ottaviani, K. N. Tu, and J. W. Mayer, Phys. Rev. Letters *44*, 284 (1980).

18. J. L. Freeouf, G. W. Rubloff, P. S. Ho, and T. S. Kuan, *Phys. Rev. Letters* **43**, 1836 (1979).
19. J. L. Freeouf, G. W. Rubloff, P. S. Ho, and T. S. Kuan, *Proc. of the 7th Annual Conf. on the Physics of Compound Semiconductor Interfaces, J. Vac. Sci. Technol.* (in press).
20. G. W. Rubloff, P. S. Ho, J. E. Lewis, V. L. Moruzzi, A. R. Williams, and C. D. Gelatt, Jr., to be published.
21. G. W. Rubloff, *Proc. of the 8th Int. Vacuum Congress/4th Int. Conf. on Solid Surfaces/3rd European Conf. on Surface Science, Cannes, France, Sept. 22-26, 1980*, to be published.
22. P. S. Ho, G. W. Rubloff, J. E. Lewis, V. L. Moruzzi, and A. R. Williams, *Phys. Rev. B* (in press).
23. Commercially available as the IBM 7406 Device Coupler.
24. P. S. Ho, T. Y. Tan, J. E. Lewis, and G. W. Rubloff, *J. Vac. Sci. Technol.* **16**, 1120 (1979).
25. D. E. Eastman, F. J. Himpsel, J. A. Knapp, and K. C. Pandey, *Proc. of the 14th International Semiconductor Conference, Edinburgh, Scotland, September 1978*.
26. F. J. Himpsel and D. E. Eastman, *Phys. Rev.* **18**, 5236 (1978).
27. W. D. Buckley and S. C. Moss, *Solid State Electronics* **15**, 1331 (1972).
28. U. Köster, K. N. Tu, and P. S. Ho, *Appl. Phys. Letters* **31**, 634 (1977).
29. F. J. Himpsel and D. E. Eastman, *J. Vac. Sci. Technol.* **16**, 1297 (1979).
30. D. E. Eastman and W. D. Grobman, *Phys. Rev. Letters* **30**, 177 (1973).
31. C. Norris, *J. Appl. Phys.* **40**, 1396 (1969).
32. S. Weng and M. El-Batanouny, *Phys. Rev. Letters* **44**, 612 (1980).
33. W. Gaebler, K. Jacobi, and W. Ranke, *Surface Science* **75**, 355 (1978).
34. W. F. Egelhoff, Jr., and G. G. Tibbetts, *Phys. Rev. B* **19**, 5028 (1979); G. G. Tibbetts and W. F. Egelhoff, Jr., *J. Vac. Sci. Technol.* **16**, 661 (1979).

35. G. Heiland and H. Lamatsch, *Surface Science* 2, 18 (1964).
36. Most reported measurements (derived mainly from UPS studies) agree with this value, including: F. G. Allen and G. W. Gobeli, *J. Appl. Phys.* 35, 597 (1964); M. Erbudak and T. E. Fischer, *Phys. Rev. Letters* 29, 732 (1972); J. E. Rowe, *Physics Letters* 46A, 400 (1974); J. E. Rowe, H. Ibach, and H. Froitzheim, *Surface Science* 48, 44 (1975); and W. Monch, *Surface Science* 63, 79 (1977). The origin of the value 0.55 eV from UPS measurements given in Ref. 3 remains unclear. In contrast, much lower values have been deduced from surface photovoltage spectroscopy (0.36 eV, J. Clabes and M. Henzler, *Phys. Rev. B* 15 21, 625 (1980)) and from photoemission threshold measurements (0.3 eV, C. Sebenne, D. Boimont, G. Guichar, and M. Balkanski, *Phys. Rev. B* 15 12, 3280 (1975)). The source of these differences is not fully understood at present. For the purposes of discussion, we use the UPS value of 0.79 eV.
37. K. Oura, S. Okada, and T. Hanawa, *Appl. Phys. Lett.* 35, 705 (1979).
38. P. S. Ho, H. Foll, J. E. Lewis, and P. E. Schmid, *Proc. of the 8th Int. Vacuum Congress/4th Int. Conf. on Solid Surfaces/3rd European Conf. on Surface Science*, Cannes, France, Sept. 22-26, 1980, to be published.
39. H. Foll, P. S. Ho, and K. N. Tu, to be published.
40. K. Pandey, to be published.
41. S. R. Nagel, G. B. Fisher, J. Tauc, and B. G. Bagley, *Phys. Rev. B* 13, 3284 (1976).
42. J. D. Riley, L. Ley, J. Azoulay, and K. Terakura, *Phys. Rev. B* 20, 776, (1979).
43. P. Oelhafen, M. Liard, H.-J. Güntherodt, K. Berresheim, and H. D. Polaschegg, *Solid State Commun.* 30, 641 (1979).
44. B. J. Wacławski and D. S. Boudreaux, *Solid State Commun.* 33, 589 (1980).
45. A. Nylund, *Acta Chem. Scand.* 20, 2381 (1966).
46. Since we have not measured $a_0/2$ vs. thickness for Pd_2Si on $\text{Si}(100)$, we cannot at present rule out the possibility that the $a_0/2$ variations on $\text{Si}(111)$ result from strain at the epitaxial interface and are unrelated to the d-peak shifts. The d-band deformation

potentials (energy shift per unit strain) in this case would have plausible values as compared to the range of optical (interband) deformation potentials of solids; see, e.g., M. Cardona, *Modulation Spectroscopy* (Academic Press, N. Y., 1969).

47. J. L. Freeouf, *Solid State Commun.* **33**, 1059 (1980).
48. W. Schottky, *Zeitschrift für Physik* **118**, 539 (1942).
49. N. W. Cheung and J. W. Mayer, to be published in *Appl. Phys. Letters*.
50. J. A. Roth and C. R. Crowell, *J. Vac. Sci. Technol.* **15**, 1317 (1978); see also J. A. Roth, Ph.D. Dissertation, Univ. of Southern Calif. (June 1979).
51. W. E. Spicer, I. Lindau, P. Skeath, C. Y. Su, and P. Chye, *Phys. Rev. Letters* **44**, 420 (1980).
52. J. O. Olowafe, P. S. Ho, H. J. Hovel, J. E. Lewis, and J. M. Woodall, *J. Appl. Phys.* **50**, 955 (1979).
53. D. E. Eastman and J. L. Freeouf, *Phys. Rev. Letters* **34**, 1624 (1975).
54. A. Hiraki, K. Shuto, S. Kim, W. Kammura, and M. Iwami, *Appl. Phys. Letters* **31**, 611 (1977).
55. I. Lindau, P. W. Chye, C. M. Garner, P. Pianetta, C. Y. Su, and W. E. Spicer, *J. Vac. Sci. Technol.* **15**, 1332 (1978).
56. L. J. Brillson, R. Z. Bachrach, R. S. Bauer, and J. C. McMenamin, *Phys. Rev. Letters* **42**, 397 (1979).

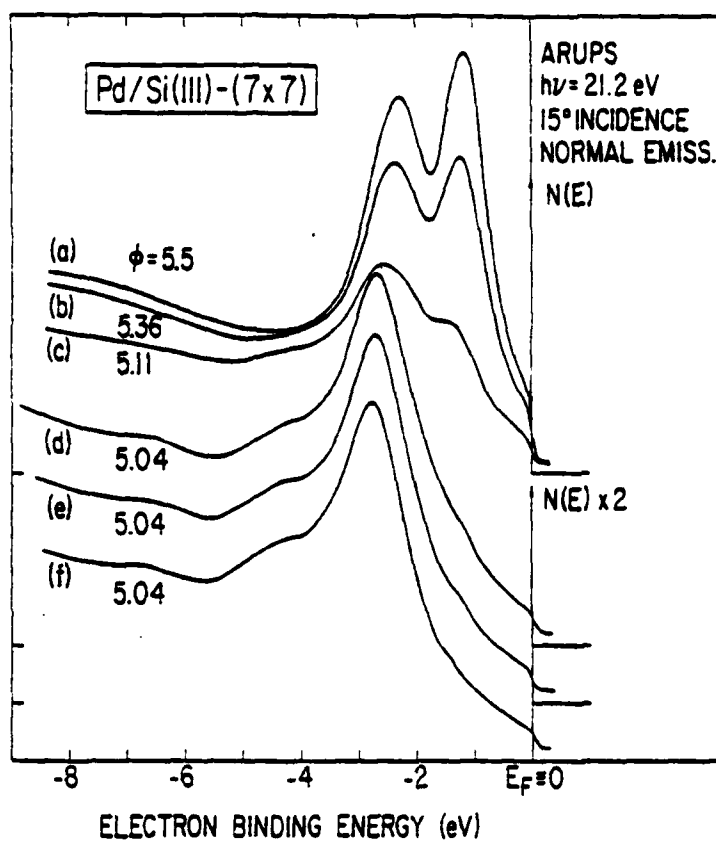


Fig. 1. a) ARUPS spectrum for $\sim 300\text{\AA}$ Pd deposited on Si(111) at 25°C ; (b)-(f) subsequent spectra taken after stepwise annealing cycles of 30 sec at 150°C .

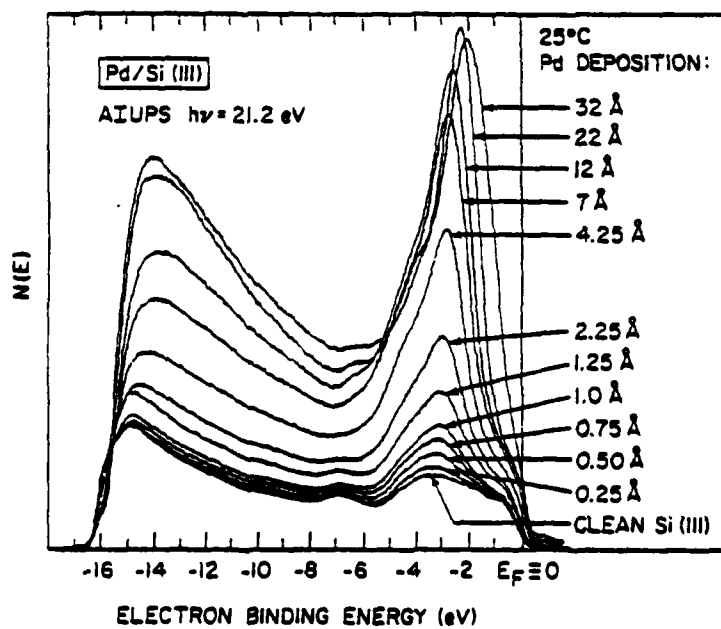


Fig. 2. AIUPS spectra for the clean Si(111) surface and for various Pd coverages deposited at room temperature.

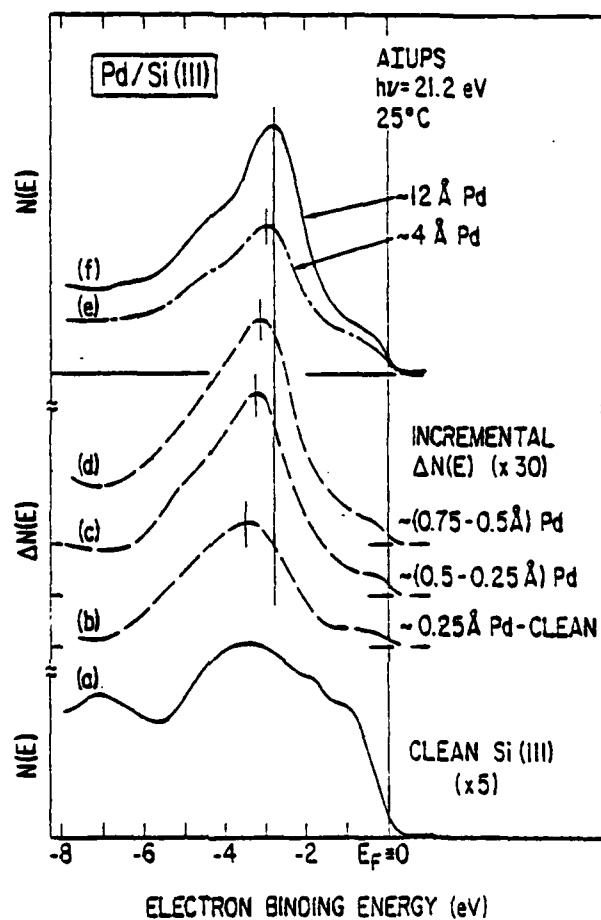


Fig. 3. AIUPS incremental difference curves for (b) 0.25 \AA Pd-covered surface minus clean Si(111) surface, (c) 0.5 \AA minus 0.25 \AA Pd-covered surfaces, (d) 0.75 \AA minus 0.5 \AA Pd-covered surfaces, and AIUPS spectra for (a) clean Si(111), (e) $\sim 4 \text{ \AA}$ Pd on Si(111), and (f) $\sim 12 \text{ \AA}$ Pd on Si(111).

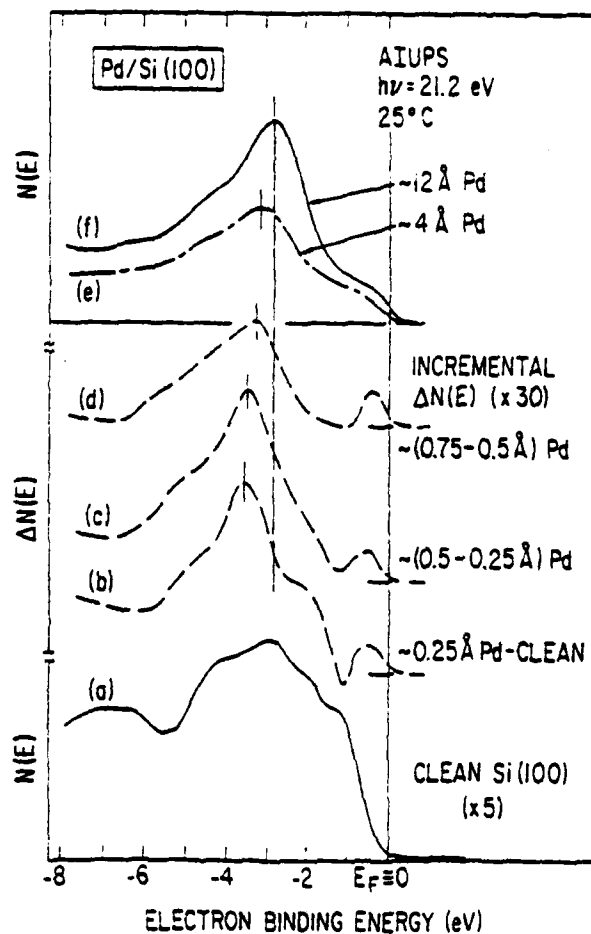


Fig. 4. AIUPS incremental difference curves for (b) 0.25 \AA Pd-covered surface minus clean Si(100) surface, (c) 0.5 \AA minus 0.25 \AA Pd-covered surfaces, (d) 0.75 \AA minus 0.5 \AA Pd-covered surfaces, and AIUPS spectra for (a) clean Si(100), (e) $\sim 4 \text{ \AA}$ Pd on Si(100), and (f) $\sim 12 \text{ \AA}$ Pd on Si(100).

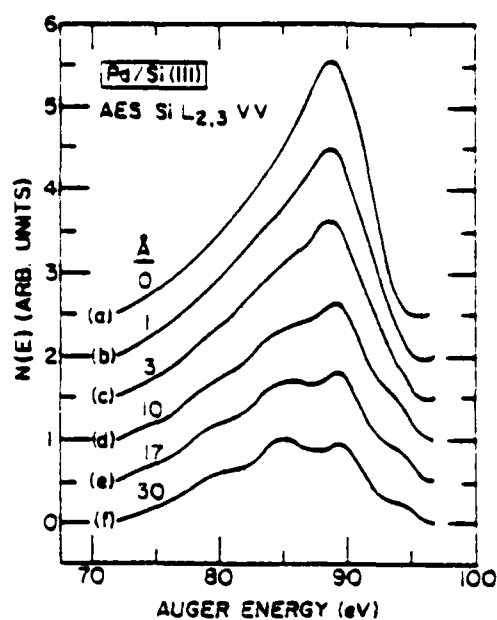


Fig. 5. Si L_{2,3} VV AES $N(E)$ spectra for (a) the clean Si(111) surface and for increasing Pd coverages (b) 1 Å, (c) 3 Å, (d) 10 Å, (e) 17 Å, (f) 30 Å.

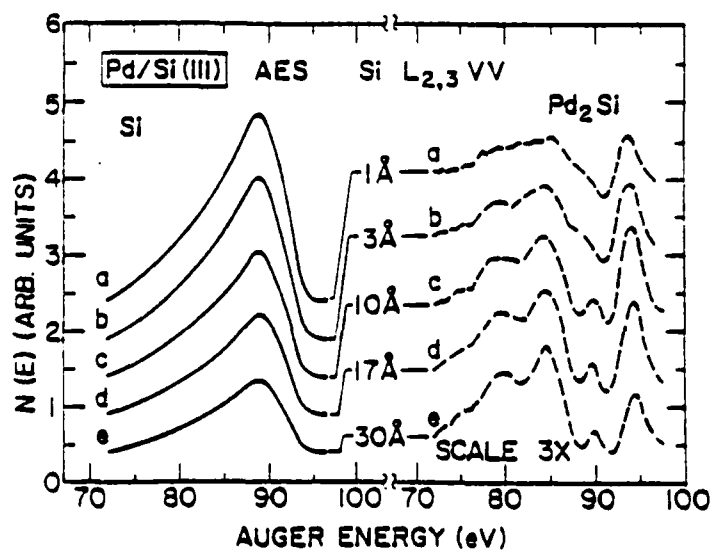


Fig. 6. Decomposition of the Si L_{2,3} VV AES spectra for Fig. 5 into Pd₂Si and elemental Si contributions.

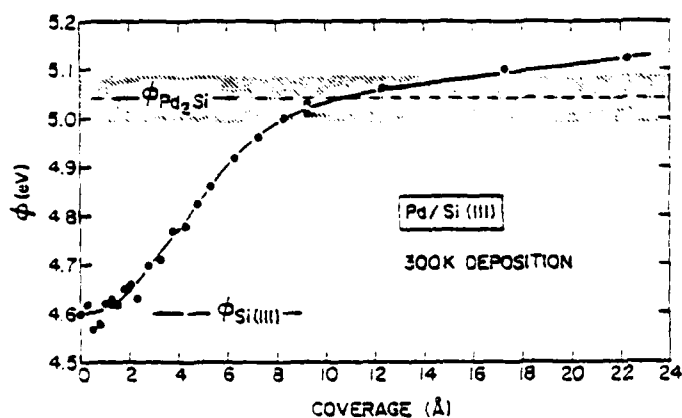


Fig. 7. Coverage-dependence of the work function (measured by AIUPS) for Pd deposited on Si(111) at room temperature. The region of Pd_2Si work function is indicated by the shaded area.

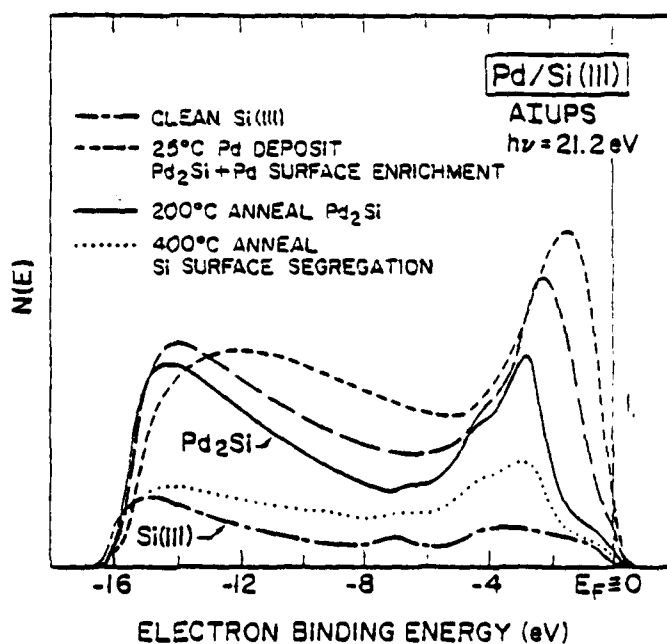


Fig. 8. AIUPS spectra:

- (i) dot-dash curve—the clean Si(111) surface;
- (ii) dashed curves—the "under-reacted" Pd_2Si surface, i.e. Pd_2Si enriched at the surface by excess unreacted Pd metal;
- (iii) solid curve— Pd_2Si (surface and bulk), formed by 200°C annealing;
- (iv) dotted curve—the "over-reacted" Pd_2Si surface, i.e. Si-enriched by Si surface segregation.

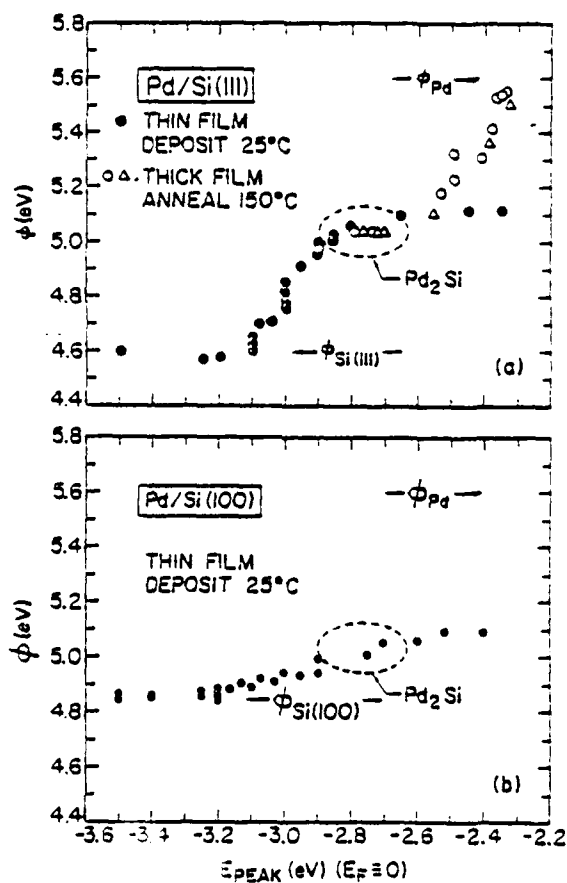


Fig. 9. Work function vs. d-band peak position from UPS as obtained from thin film deposition steps at 25°C (solid dots) and from thick film annealing (150°C) steps (open circles and triangles). The plateau regions (surrounded by dashed line) near $E_{\text{PEAK}} = -2.75$ eV and $\phi = 5.04$ eV indicates where the surface is essentially Pd_2Si , like the underlying bulk.

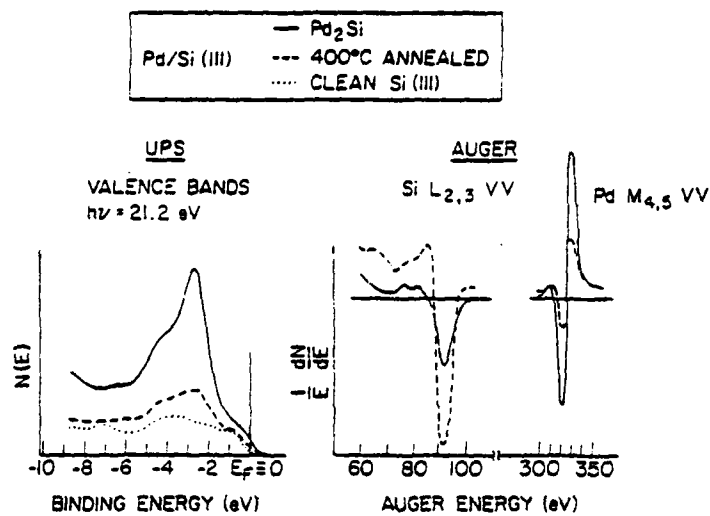


Fig. 10. Si surface segregation effects on Pd_2Si surface spectra induced by 400°C annealing ("over-reaction").

RC 8285 (#36047) 5/21/80
Solid State Physics 16 pages

Cross-Sectional TEM of Silicon-Silicide Interfaces*

H. Föll, P. Ho, K.N. Tu

IBM, T.J. Watson Research Center

Yorktown Heights, N.Y. 10598

U.S.A.

Typed by L. Miro

ABSTRACT:

The epitaxial interfaces of Si/Pd₂Si, Si/NiSi₂, and to a lesser extent Si/PtSi have been investigated by TEM using cross-sectional specimens. Direct lattice imaging was used to image the Si/Pd₂Si and the Si/NiSi₂ interfaces. The Si/Pd₂Si interface was found to be rather smooth on a macroscopic scale but rough on an atomic scale whereas the opposite is true for the Si/NiSi₂ interface. A twinning relationship between NiSi₂ and {111} Si has been observed. The Si/PtSi interface is very rough on a macroscopic scale. Interface dislocations are present in the Pd- and Ni-Silicide cases. No evidence for an amorphous interfacial layer has been obtained.

To be published in J. Appl. Phys.

*Supported in part by the Office of Naval Research

I INTRODUCTION

Thin films of silicides find increasing use as ohmic or Schottky contacts in Si devices. This is not only because the silicide/Si interface has electrical properties suitable for contacts to very small junctions but also because the silicide layer can improve junction reliability by providing an effective barrier against Al-penetration into the junction.¹ Silicides are commonly formed by a solid-state reaction between the Si substrate and an evaporated metal film. During the reaction the silicide/Si interface moves into the Si thus providing a relatively clean interface which is not much affected by the native oxide or any contamination on the original Si surface. For optimal junction characteristics, a uniform and relatively flat interface is required, therefore the knowledge on the interface morphology is important. Moreover, there exists a considerable basic interest in the atomic structure of the silicide/Si interface. For example, the formation of the first phase and the electronic properties of the contact might be controlled by the atomic structure of the interface¹. The existence of a thin amorphous metallic glass at the interface has been proposed in order to predict the formation of the first silicide phase in transition metal/Si systems². A direct observation of the atomic structure of silicide/Si interfaces, however, has not been reported so far. This is because the methods commonly used to study silicides, e.g. ion back scattering and glancing angle x-ray diffraction cannot provide a detailed information about interface properties on an atomic scale. A more suitable method for studying these

properties is transmission electron microscopy (TEM), particularly with specimens prepared for a cross-sectional examination. This paper gives first results of such a TEM investigation. The silicides chosen for this study were near-noble metal silicides: Pd_2Si , NiSi_2 and PtSi which can grow epitaxially on Si thus facilitating a detailed structural observation by TEM lattice imaging techniques.

II. EXPERIMENTAL

The silicides studied were: Pd_2Si on chemically cleaned {111} surfaces, NiSi_2 on chemically cleaned {100} and {111} surfaces and, to a lesser extent, PtSi on chemically cleaned {111} surfaces. All silicides were formed by electron-beam evaporation of the metals at room temperature followed by an annealing treatment either in vacuum or in He atmosphere.

After the silicides were formed, specimens with dimensions of approximately $2 \times 2 \times 5\text{mm}$ were cut from the wafers. Several of these specimens were then glued together using Araldite or Epon epoxy, following the procedure outlined by Sheng and Chang³. During the curing of the epoxy the specimen block was kept under pressure in a small, teflon-lined press to insure a thin and uniform epoxy layer between the specimens. From this specimen block thin slices were cut with a wire saw and subsequently ground and polished to a final thickness of $\sim 50\mu\text{m}$. These slices were then glued on a supporting Cu grid with one large hole and finally ion-milled at $\sim 5\text{kV}$ from

both sides until a hole was formed in the sample center. In order to obtain good specimens it is important to start with a rather thin specimen ($\sim 50\mu\text{m}$) and to keep the epoxy layer as thin as possible ($< 1\mu\text{m}$). Ion milling at low voltages ($\sim 1\text{kV}$) introduces damage (visible black dots) into the Si whereas at higher voltages ($\sim 5\text{kV}$) no directly visible damage was observed. Specimens for investigations of the silicide "flat-on" were made by chemical thinning of the Si from the backside. TEM was performed in a Siemens Elmiskop 102 operating at 125kV , or in a Jeol 200 B operating at 200kV .

III. RESULTS AND DISCUSSION

Palladium-Silicide

The first case to be discussed is Pd_2Si which was made by evaporating 50nm of Pd on a $\{111\}$ Si wafer; no subsequent annealing treatment was performed. Cross-sectional specimens were made and during the specimen preparation its temperature may have reached $\sim 100^\circ\text{C}$ for ~ 20 hrs during ion-milling. TEM showed that the Pd had partially reacted with Si forming a Pd_2Si layer $\sim 31\text{ nm}$ thick, the remaining Pd layer had a thickness of $\sim 37\text{ nm}$. Fig. 1 shows a cross-sectional view of this sample and illustrates very clearly some of the artifacts and difficulties encountered in cross-sectional TEM. Due to the stresses in the sample, thin areas of the specimen around the interface region are severely bent; frequently the silicide is even partially peeled off. In this case the Si and the silicide are separated by a groove which

appears as a bright band in Fig. 1. Different ion-milling rates between Pd, Pd₂Si and Si may also contribute to such artifacts. This makes it exceedingly difficult to ascertain whether some observations reflect intrinsic properties of the sample, or are due to artifacts and/or a mixture of both. The presence of voids in the interface, for example, would facilitate a peeling-off of the silicide layer; this was observed for metal layers on GaAs⁴ and may also play a role in the Pd₂Si case. Despite all these difficulties, Fig. 1 shows that the Pd₂Si is basically single crystalline and has an epitaxial relationship to the Si matrix (this was deduced from the diffraction pattern); the unreacted Pd is polycrystalline with a grain size of ~ 10-20nm. More importantly, it is clearly visible that the Si/Pd₂Si and the Pd₂Si/Pd interfaces are rather flat with an estimated roughness of ~ 2nm.

The bending of the specimen in the interface region makes direct lattice imaging of the interfacial region very difficult. For carrying out so-called structural imaging^{5,6} which under favorable conditions can give a direct information about the positions of atoms, the specimen has to be oriented very precisely into a high-symmetry orientation⁷ (in this case {110} for the Si and $\{1\bar{1}00\}$ for the Pd₂Si). This so-called axial diffraction condition can be easily achieved in the thicker parts of the Si by using Kikuchi lines, but in interface regions thin enough for lattice imaging (< 40nm for Si, < 10nm for Pd₂Si) the unavoidable bending of the specimen makes almost certain that the diffraction conditions are no longer axial. Consequently, lattice images, if

obtained at all, are no longer structural images (i.e. they cannot be interpreted in terms of absolute atom positions). Nevertheless, they still contain valuable information not obtainable otherwise. Fig. 2 shows a lattice image in the Si-Pd₂Si interface of the sample shown in Fig. 1. On the Si side, the contrast is similar to a structural image (i.e. the white dots may be interpreted as the open channels of the Si lattice viewed in the $\langle 110 \rangle$ direction*), whereas only the $\{22\bar{4}0\}$ fringes of the hexagonal Pd₂Si lattice are visible in the Pd₂Si. The interface is rough on an atomic scale with an average amplitude of $\sim 1.5\text{nm}$ and an average wavelength of $\sim 4\text{nm}$. A circuit (analogous to a Burgers circuit) going from a well resolved point at the interface on the Si side to another well resolved point at the interface and then back to the starting point in the Pd₂Si side (cf. Fig. 2) reveals the presence of excess $\{22\bar{4}0\}$ fringes in the Pd₂Si side. That is, there are more Pd₂Si $\{22\bar{4}0\}$ fringes than corresponding Si $\{111\}$ fringes (counted along the interface) within a certain distance along the interface. This indicates that dislocations are present within the circuit and since these dislocations are neither in the Si nor in the Pd₂Si (as verified by looking along the Pd₂Si $\{22\bar{4}0\}$ fringes or the Si $\{111\}$ fringes), they must be in the interface and therefore are interface dislocations. On the average, there is one additional Pd₂Si $\{22\bar{4}0\}$ fringe for about 23 Si $\{111\}$ fringes. The additional $\{22\bar{4}0\}$ fringes cannot simply be identified as partial dislocations having a Burgers vector $b = \frac{a}{6}\langle 11\bar{2}0 \rangle$ (the distance between $\{22\bar{4}0\}$

*) or, alternatively, as the product of two sets of $\{111\}$ fringes crossing each other.

planes) because lattice imaging reveals only the component of the Burgers vector in the image plane ⁸ (therefore, a dislocation with an inclined Burgers vector $b = \frac{a}{3}\langle 11\bar{2}0 \rangle$ would give the same image as $b = \frac{a}{6}\langle 11\bar{2}0 \rangle$). Moreover, the concept of dislocation in the interface between a hexagonal and a cubic material needs more detailed considerations than intended in this paper, especially if the interface is not flat but has steps, as is the case with the Pd₂Si-Si interface. Nevertheless, the presence of dislocations, whatever detailed characteristics they might have, is a strong argument for an ordered interface; i.e. no amorphous layer is present. This is already indicated by the absence of such a layer in the lattice image in Fig. 2 although in some places a very thin (< 1nm) amorphous-like layer might be obscured in this picture because the interface cannot be expected to be exactly end-on, due to its roughness.

Measuring the spacing of a large number of $\{22\bar{4}0\}$ fringes in the silicide and comparing it to the spacing of the Si $\{111\}$ fringes allows one to obtain a fairly accurate measurement of the Pd₂Si lattice constant. If the lattice constant of the Si is taken to be $a = 0.357$ nm (measured 8nm away from the interface), the Pd₂Si lattice constant is determined to be $a = 0.642$ nm (~ 1.5nm away from the interface) which is ~ 1.5% smaller than the nominal (x-ray) value of 0.652nm. This indicates the presence of elastic stresses and possibly also a change in the lattice constant of the silicide due to non-stoichiometry. A Pd-rich silicide, e.g. has been shown to lead to smaller lattice

constants compared to a stoichiometric silicide⁹ and this may also be true for Si-rich silicides. This interpretation is supported by the presence of more misfit dislocations than would have been needed to compensate for the differences in the lattice constants of Si and stoichiometric Pd_2Si , which would have been one ending $\{22\bar{4}0\}$ fringe for every 50 Si $\{111\}$ fringes. With the measured lattice constant of Pd_2Si ($a = 0.642\text{nm}$), one additional fringe for every 29 $\{111\}$ fringes of Si would be expected which agrees fairly well with the observed value of $\sim 23\text{-}25$.

The Si image close to the interface shows an intensity modulation of the lattice fringes which appears to be a Moiré contrast effect. On the average, every third Si $\{111\}$ fringe parallel to the interface is somewhat brighter than its neighbors. A contrast like this could result from overlapping crystals with similar lattice geometry but different lattice constants, e.g. at an interface inclined with respect to the electron beam. The roughness of the Pd_2Si -Si interface however cannot account for the rather broad zone of the Moiré contrast ($\sim 8\text{nm}$) since at the most a region $\sim 1\text{nm}$ in width can be expected to show this effect. While it is possible that the lattice constant of Si could be locally changed by incorporating of Pd atoms, this change would have to be in the order of 50% to explain the observed contrast; this is too high to be reasonable and the remaining possibilities to account for this contrast are: Some form of platelet-like Pd-rich regions (possibly small monolayers of Pd_2Si) or a thin surface layer of Pd_2Si which may have formed during speci-

men preparation. Some Pd might have reached the Si surface by surface migration (possibly assisted by the ion-milling process) and may have reacted to form Pd_2Si . At present, it is not possible to distinguish between these two possibilities.

Nickel Silicide

NiSi_2 was formed on both {100} and {111} Si by evaporating 50nm of Ni at room temperature and subsequent annealing at 800°C in He atmosphere. In order to form different phases of Ni silicides, part of the sample was directly annealed at 800°C for 1 hr, and another part was first annealed at 300°C for 20 min (which forms $\text{Ni}_2\text{Si}^{10}$) then at 400°C for 20 min (which forms NiSi^{10}) and finally at 800°C for 1 hr.

NiSi_2 on {100} Si

The NiSi_2 on {100} Si forms a heavily faceted interface with the Si substrate (Fig. 3). The facets are on {111} and {100} planes with the former more frequently observed. The interface is very rough on a large scale and the thickness of the NiSi_2 layer may vary by more than 100nm (the average thickness is 170nm). The NiSi_2 formed by stepwise annealing appears to be somewhat less faceted than the NiSi_2 formed by direct annealing, but the over-all difference is not significant.

On an atomic scale the interface is perfectly flat within a facet; Fig. 4 shows an example. A facet on a {100} plane and on a {111} plane can be seen and the interface was found to be confined to one lattice plane for a lateral dimension of more than 60nm (the largest distance measurable on the original negative). An off-set of the {111} fringes crossing the interface is visible in Fig. 4, but this could be a contrast artifact, however, it may also reflect a true property of the interface. A Burgers circuit similar to the one described for Pd_2Si does not reveal interface dislocations in Fig. 4, but this cannot be taken as evidence for the absence of misfit dislocations since the area sampled might have been too small. In fact, if a cross-sectional sample is tilted about an axis not perpendicular to the interface (so the interface is no longer end-on) interfacial dislocations, and dislocations in the silicide are visible (Fig. 5). These dislocations can be better revealed using conventional TEM techniques with the electron beam normal to the sample surface. Fig. 6 gives such an example. Due to the stresses present in the sample, the specimen starts to bend severely as soon as it becomes thin enough for TEM, this practically prevents the imaging using a well-defined diffraction condition. Despite this difficulty, three basic types of dislocation networks have been distinguished: 1) a square network of edge dislocations with $b = \frac{a}{2} \langle 110 \rangle$, and with a spacing of $\sim 57\text{nm}$, 2) a hexagonal network with a spacing similar to that given above and probably also containing edge dislocations with $b = \frac{a}{2} \langle 110 \rangle$, and 3) a rather irregular rectangular network with a spacing from 50nm-200nm. These networks can be accounted for simply by assuming that

in the first case the dislocation network is on a rather large {100} facet; in the second case on a large {111} facet and in the third case on an area with many small facets. The observed spacing of $\sim 57\text{nm}$ is considerably smaller than the theoretically expected value of $\sim 97\text{nm}$ taking the lattice constant of NiSi_2 to be $a = 0.5406\text{nm}$ ¹⁰. This indicates that the difference in lattice constants is larger at 800°C so that more misfit dislocations are needed to relieve the stresses. During cooling down of the wafers the dislocations were frozen-in thus creating the high stresses observed at room temperatures.

NiSi_2 on {111} Si

The interface between {111} Si and NiSi_2 is also faceted, but much less so than on {100} Si. Fig. 7 shows a typical example where it can be seen that very large facets are formed on the {111} plane parallel to the original wafer surface and only small facets are found on the inclined {111} planes. The amplitude of interface roughness is $\sim 20\text{nm}$ with a rather large modulation period in the order of several μm . In this case it was also found that the surface of the NiSi_2 was faceted; see insert in Fig. 7. Direct lattice imaging again showed a perfectly straight interface which can be defined within one {111} plane, see Fig. 8. However, as can be seen in Fig. 8, the NiSi_2 is not epitaxial to the Si matrix but rather in a twin orientation relative to the Si; this is also shown by the twin spots in the diffraction pattern. The direct lattice image, however, has the advantage of demonstrating that the entire silicide is twinned and that the twin spots do not come from micro-twins

within an epitaxial silicide. Burgers-circuits in some of direct lattice images as the well as the images of tilted specimen, Fig. 9, show the presence of dislocations at the interface. Again, conventional (flat-on) specimens are better suited for studies of such networks and Fig. 10 gives an example. It should be mentioned, however, that images observed on strongly tilted cross-sectional specimens show directly that the network is at, or very close to the interface (Figs. 5,9), an information not easily obtainable with conventional techniques. A rather regular hexagonal network with a spacing of $\sim 50\text{nm}$ can be seen in Fig. 10 which is interrupted in some places by patches of a less regular hexagonal network with a spacing of $\sim 85\text{nm}$. Contrast analysis showed that the network with the smaller spacing consists of edge dislocations with $b = \frac{a}{6}\langle 112 \rangle$ whereas the larger network is formed by edge dislocations with $b = \frac{a}{2}\langle 110 \rangle$. The latter marks the areas where NiSi_2 has grown in a direct epitaxial relationship to the matrix, whereas the former is formed in the twin boundary between the Si and the NiSi_2 . The spacing of the dislocations in these cases is closer to the theoretically expected value ($\sim 97\text{nm}$ for $b = \frac{a}{2}\langle 110 \rangle$ dislocations and $\sim 60\text{nm}$ for $b = \frac{a}{6}\langle 112 \rangle$), indicating a better fit at 800°C between NiSi_2 and $\{111\}\text{Si}$ than between NiSi_2 and $\{100\}\text{Si}$. The dislocation nodes in the network of the perfect dislocations may be somewhat extended, but no clearcut statement can be made at present. About 80% of the total area showed the twin-related network, indicating that a twinned interface is strongly preferred. The misfit dislocations with $b = \frac{a}{6}\langle 112 \rangle$ are the grain-boundary dislocations expected for a twin boundary, which for

topological reasons can only exist exactly in the twin boundary, i.e. in the interface. Again, this is a clear evidence for an ordered interface without an amorphous interface layer, in contrast to recent predictions^{2,12}.

Platinum Silicide

Only one specimen has been investigated. PtSi was formed by deposition of 500nm Pt at room temperature on {111} Si and by a subsequent heat treatment at 400°C for 2 hrs. This specimen was of particular interest because the PtSi layer showed fine lines concentric to the center of the wafer. Conventional TEM showed that the PtSi grains in these lines (width ~ 1 μ m) were almost randomly oriented with respect to the matrix, whereas between the lines they were in an pseudo-epitaxial relationship with respect to the Si¹³. It is possible that the circular lines in the silicide reflect areas of the Si wafer where some residual damage or contamination from the last polishing step was present. Cross-sectional specimens showed that the Si-PtSi pseudo-epitaxial interface is exceedingly rough, with amplitudes of 200nm (thickness ~ 350nm) and a wavelength of ~ 700nm (Fig. 11). In contrast, the PtSi surface is rather flat. This example serves to demonstrate that epitaxial interfaces are not necessarily flat.

IV CONCLUSIONS

Transmission electron microscopy of silicon-silicide interfaces with cross-sectional specimens is a powerful technique for studying interfacial properties

at high spatial resolution. Interfacial parameters such as flatness, preferred interfacial planes, and interfacial defects are easily observable and can be measured almost at an atomic level. It was found that the Si/Pd₂Si interface is rough on an atomic scale and that it contains interfacial dislocations. The NiSi₂/Si interface is faceted but perfectly flat on an atomic scale. NiSi₂ grows epitaxial on {100} Si, but has a twin-relation to {111} oriented Si. No evidence for an amorphous interface layer was found in either case.

REFERENCES

1. K.N. Tu and J.W. Mayer in "Thin Films - Interdiffusion and Reactions," edited by J.M. Poate, K.N. Tu and J.W. Mayer, (John Wiley, New York, 1978) p. 359.
2. R.M. Walser and R.W. Bené, Appl. Phys. Lett. 28, 624 (1976).
3. T.T. Sheng and C.C. Chang, IEEE Trans. Elect. Devices, 23, 531 (1976).
4. C.C. Chang, T.T. Sheng, R.J. McCoy, S. Nakahara and F. Ermanis, J. Appl. Phys. 50, 7030 (1979).
5. J.C.H. Spence, M.A. O'Keefe and H. Kolar, Optik 49, 307 (1977).
6. A. Bourret, A. Renault and G.R. Anstis, Chemica Scripta 14, 207 (1979).
7. W.D. Buckley and S.C. Moss, Solid State Electr., 15, 1331 (1972).
8. D.J.H. Cokayne, J.R. Parsons and C.W. Hoelke, Phil Mag. 24, 139 (1971).
9. T.S. Kuan and J.L. Freeouf, in "Proc. 37th EMSA meeting" (Claitor's, Baton Rouge) p. 696 (1979)

10. K.N. Tu, E.I. Alessandrini, W.K. Chu, H. Kraulte and J.W. Mayer, Jap. J. Appl. Phys. Suppl. 2, Pt. 1, 669 (1974).
11. W. Bollmann: "Crystal defects and crystalline interfaces" (Springer Verlag 1970).
12. W.J. Schaffer, R.W. Bene' and R.M. Walser, J. Vac. Sci. Technol., 15, 1325 (1978).
13. A.K. Sinha, R.B. Marcus, T.T. Sheng and S.E. Haszko, J. Appl. Phys. 43, 3637 (1972).



Fig. 1. Thin layer of Pd₂Si and Pd on Si. The layer is severely bent (coming out of the paper plane in the left-hand corner).

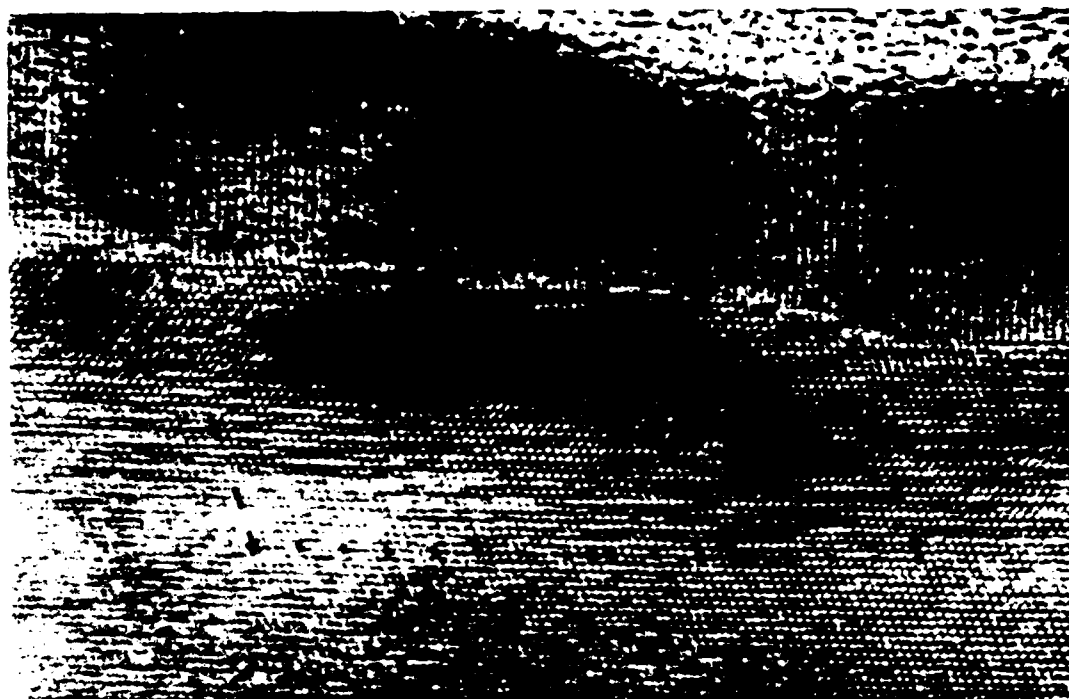


Fig. 2. Lattice image of the $\text{Pd}_2\text{Si-Si}$ interface. The spacing of the Si $\{111\}$ fringes (e.g. parallel to the interface) is 0.31 nm. A Burgers-like circuit is drawn in, showing 79 $\text{Pd}_2\text{Si}\{22\bar{4}0\}$ fringes for 75 Si $\{111\}$ fringes.

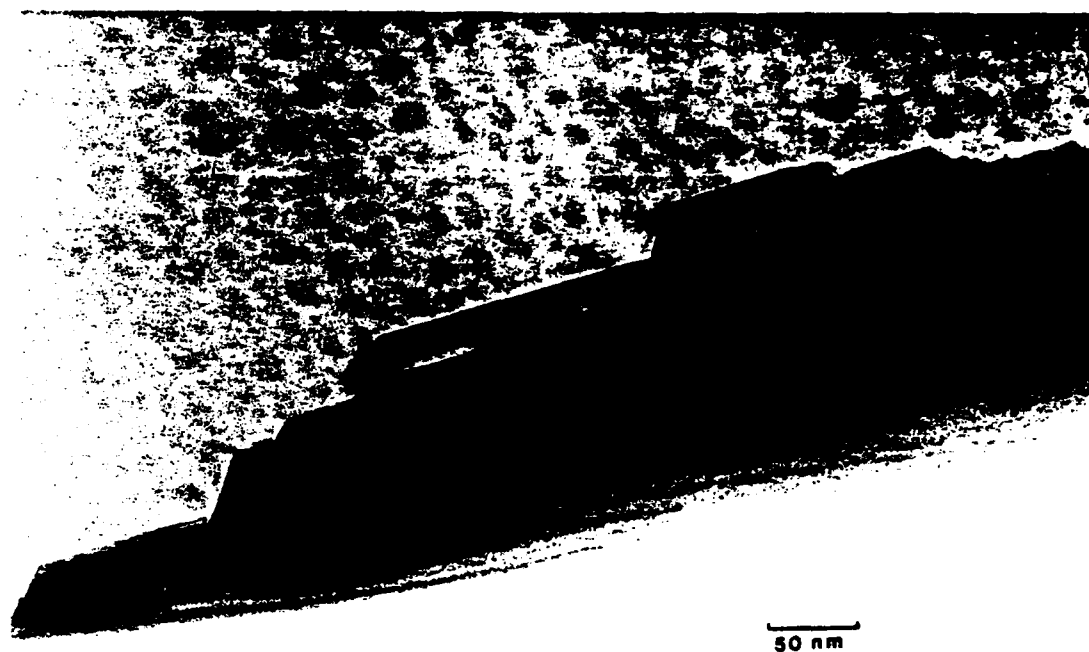


Fig. 3. Heavily faceted NiSi_2 on $\{100\}$ Si. Parts of the silicide have been removed during ion-milling; the surface of the silicide therefore is not the original silicide surface.

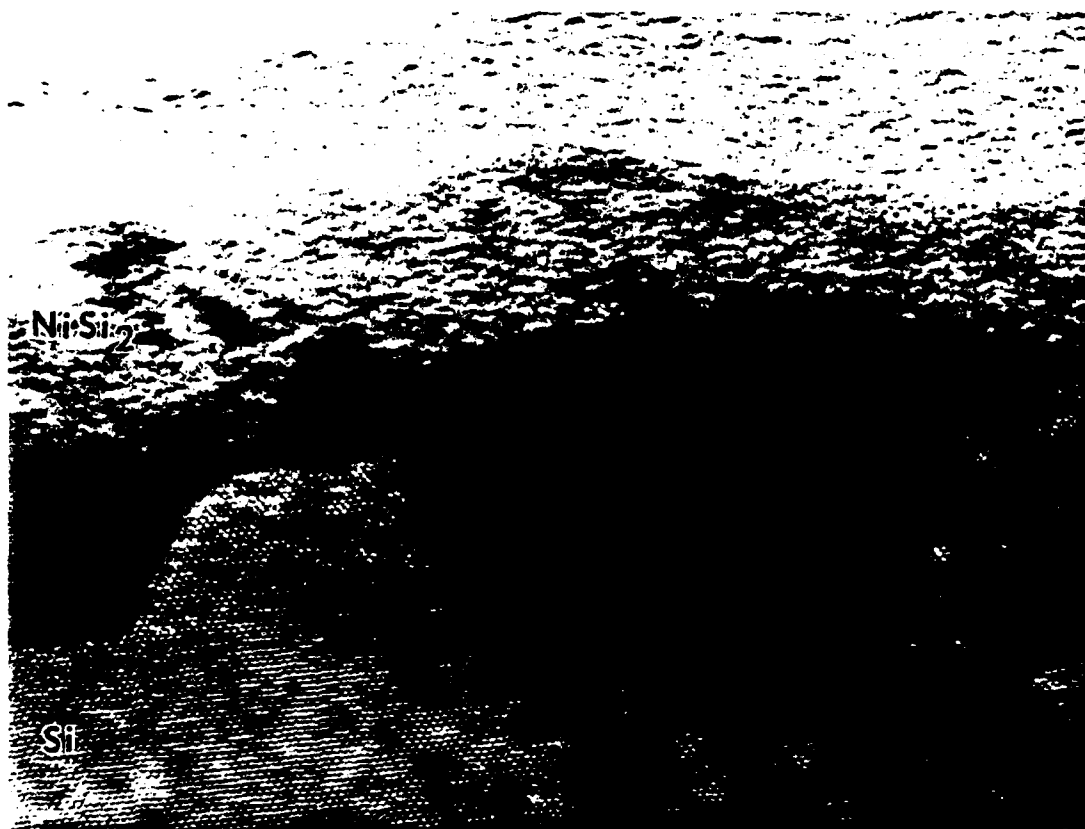


Fig. 4. Lattice image of the Si-NiSi₂ interface for silicide formed on {100} Si. A large facet ^{on} a {100} plane and a small facet on a {111} plane are visible.

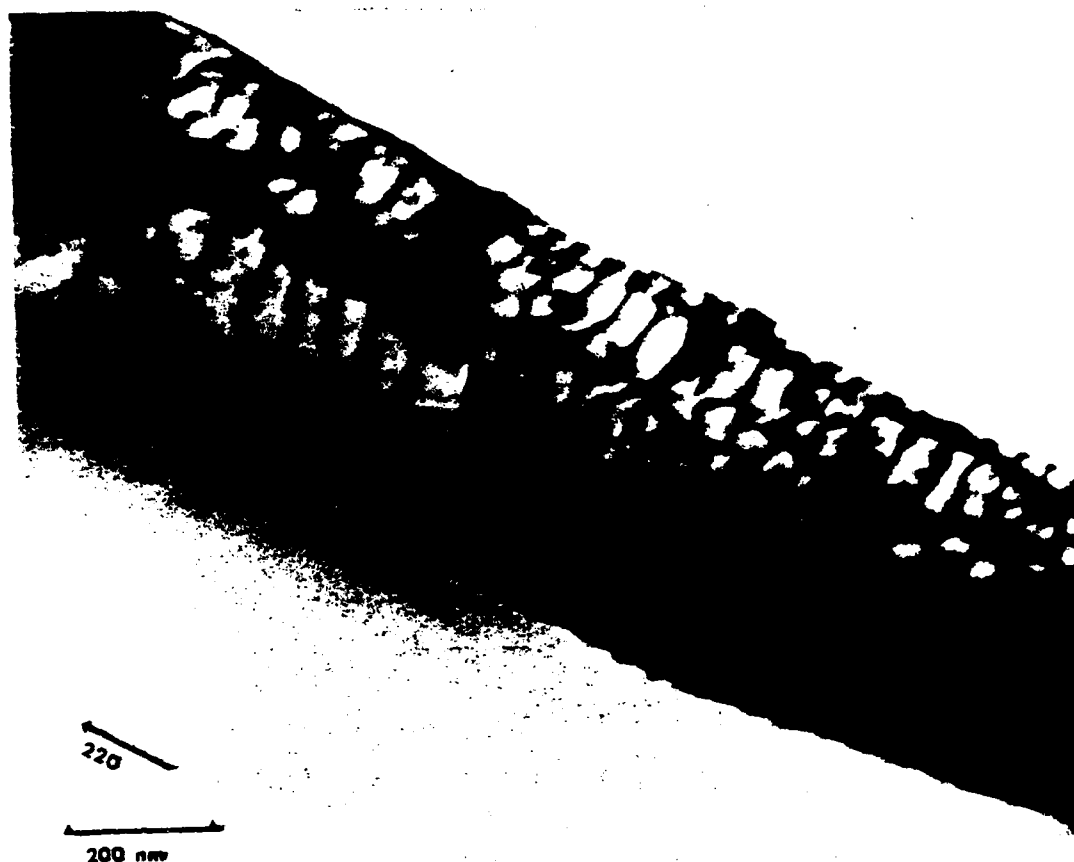


Fig. 5. Misfit dislocations in the Si-NiSi₂ {100} interface and dislocations in the silicide.

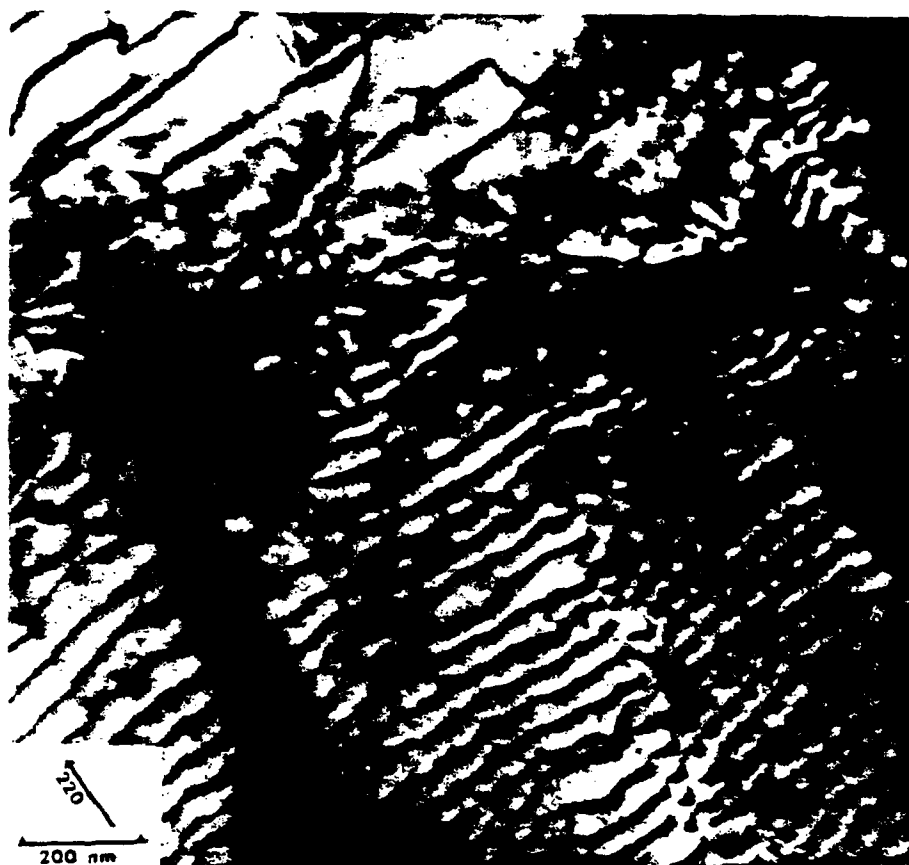


Fig. 6. Misfit dislocations in the Si-NiSi₂ interface viewed flat-on. A hexagonal network (lower right-hand corner; one set of dislocations not in contrast), a square network (left-hand corner; one set of dislocations not in contrast) and on irregular rectangular network can be seen.

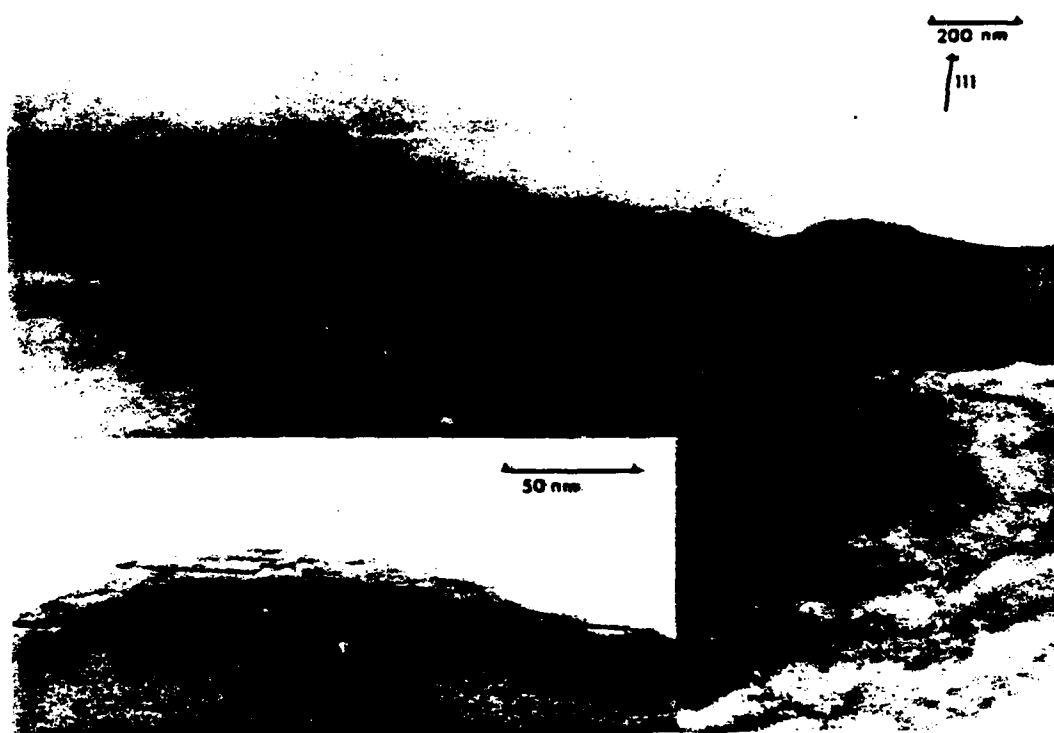


Fig. 7. Interface between NiSi_2 and $\{111\}$ Si. The insert shows the NiSi_2 surface at higher magnification.



Fig.8. Lattice image of the Si-NiSi₂ interface on a {111} plane. The NiSi₂ is twinned with respect to the Si matrix; this also can be seen from the typical twin diffraction pattern. The interface contains a dislocation at the dark spot.



Fig. 9. Misfit dislocations in the interface between NiSi_2 and $\{111\}$ Si.



Fig. 10. Flat-on view of misfit dislocations in the Si-NiSi₂ {111} interface. The micrograph was taken with multi-beam diffraction conditions close to the {111} pole.



Fig. 11. Interface between Si and PtSi (two samples with the silicide side glued together).

END